Evolution of Weakly Nonlinear Water Waves in the Presence of Viscosity and Surfactant

S.W. Joo, A.F. Messiter* and W.W. Schultz
Department of Mechanical Engineering and Applied Mechanics
*Department of Aerospace Engineering

Contract Number N00014-86-K-0684
Technical Report No. 89-07

August, 1989

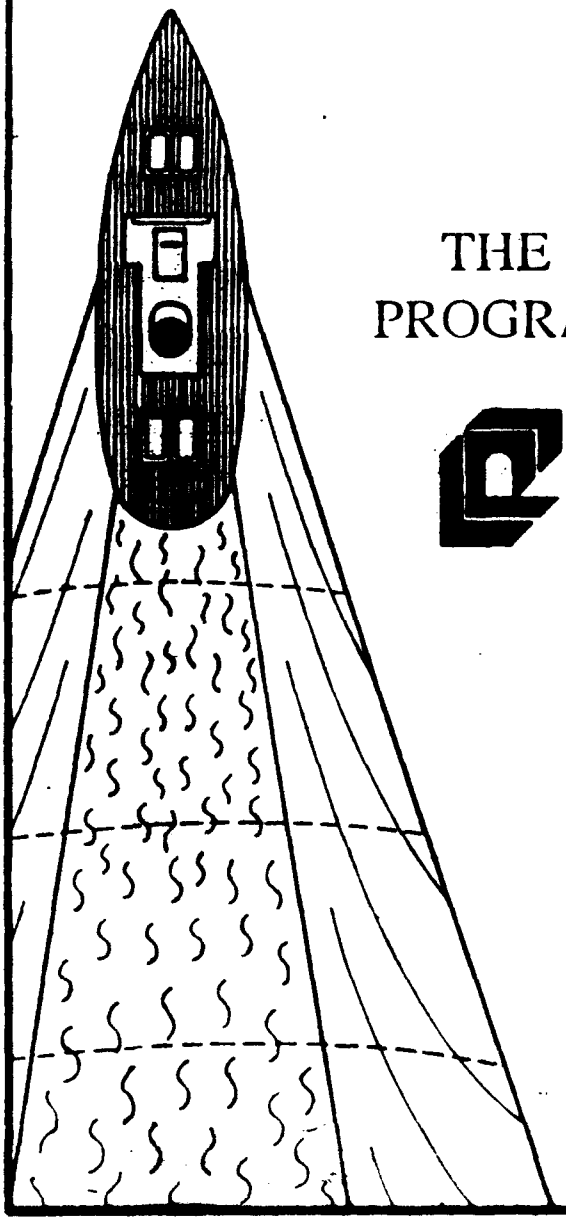

THE UNIVERSITY OF MICHIGAN
PROGRAM IN SHIP HYDRODYNAMICS

COLLEGE OF ENGINEERING

NAVAL ARCHITECTURE &
MARINE ENGINEERING

AEROSPACE ENGINEERING

MECHANICAL ENGINEERING &
APPLIED MECHANICS

SHIP HYDRODYNAMIC
LABORATORY

SPACE PHYSICS RESEARCH
LABORATORY

ERIM

Evolution of Weakly Nonlinear Water Waves in the Presence of Viscosity and Surfactant

S. W. Joo, A. F. Messiter* and W. W. Schultz
Department of Mechanical Engineering and Applied Mechanics,
University of Michigan, Ann Arbor, Michigan 48109

*Department of Aerospace Engineering,
University of Michigan, Ann Arbor, Michigan 48109

August 14, 1989

ABSTRACT

Amplitude evolution equations are derived for viscous gravity waves and for viscous capillary-gravity waves with surfactants in water of infinite depth. Multiple scales are used to describe the slow modulation of a wave packet, and matched asymptotic expansions are introduced to represent the viscous boundary layer at the free surface. The resulting dissipative nonlinear Schrödinger equations show that the largest terms in the damping coefficients are unaltered from previous linear results up to third order in the amplitude expansions. The modulational instability of infinite wavetrains of small but finite amplitude is studied analytically and computationally. For capillary-gravity waves a band of Weber numbers is found in which the linear analysis guarantees neutral stability in the absence of viscous dissipation. The corresponding spectral computation shows modulation features that represent a small-amplitude recurrence not directly related to the Benjamin-Feir instability.

1 Introduction

Although water waves are adequately described by inviscid-flow theory in most cases, the effects of viscosity and interfacial properties become important for waves of short wavelength. For sufficiently short waves, the shear-stress boundary condition, which is neglected in classical studies, must then be satisfied at the free surface. If the free surface is clean and the air above is ignored, the shear stress vanishes. However, when a layer of contaminant (surfactant) is present on the free surface, its concentration varies in accordance with the motion of the free surface, causing a surface-tension gradient that must be balanced by a nonzero surface shear stress. Therefore, the characteristics of the surfactant must be examined before the boundary conditions can be prescribed completely.

The highly dissipative effect of surfactants has been observed since classical times (see Pliny, 77 A.D., for example). A qualitative explanation of its cause in terms of the variations in surface tension was given by Reynolds (1880), as cited by Lamb (1932). Levich (1941, 1962) later performed a more thorough analysis, and an extension of this work was described in the review of Lucassen-Reynders & Lucassen (1969). In these mathematical models the surfactant was considered as an interfacial film of infinitesimal thickness. Closed-form solutions for the damping coefficient were given for linear capillary waves, and the damping effect was shown to increase dramatically from that for a clean surface. A series of more complicated models proposed by Goodrich (1960, 1962) treated the surfactant as an anisotropic rheological body. A simpler viscoelastic interfacial constitutive equation that compared favorably with experimental measurements was developed by Addison & Schechter (1979). Extensive references describing the various effects of surfactants on water waves were given by Lucassen (1982) and Garrett (1986).

In the aforementioned investigations, the study of viscous damping associated with water waves has been confined to linear theory, in which the wave amplitude is infinitesimal and the free-surface boundary conditions are applied at a mean surface. In the present work, we focus on the wave nonlinearity and adopt the simple elastic model of Lucassen-Reynders & Lucassen

(1969) and Lucassen (1982), which is suitable for many insoluble surfactants.

The usual theory of weakly nonlinear waves is based on the assumptions that the fluid is inviscid and the motion is irrotational. Of particular interest are solutions that address the evolution of a wave packet and the instability of a Stokes wavetrain. Benjamin & Feir (1967) and Whitham (1967) demonstrated in different ways that progressive waves of finite amplitude on deep water are unstable. The evolution equation for the slowly varying amplitude is a nonlinear Schrödinger equation (NLS), first introduced for water waves by Zakharov (1968) with a variational method and obtained by Hasimoto & Ono (1972) using the method of multiple scales. Peregrine (1983) summarized various analytical solutions to the NLS equation, and Yuen & Ferguson (1978), Weideman & Herbst (1987), and many others studied numerical solutions. An extension to three-dimensional wave packets was given by Davey & Stewartson (1974), and capillary effects were considered by Djordjevic & Redekopp (1977). The damping effect has been included in the two-dimensional NLS equation, e.g., by Pereira & Stenflo (1977), through the addition of a conjectured small dissipation term. A primary objective of the present work is to develop a systematic derivation of the amplitude equation in the presence of viscosity and a thin surfactant film. The result is a dissipative nonlinear Schrödinger equation (dissipative NLS), which contains a linear dissipation term; the other terms remain unaltered from their counterparts for inviscid flow.

We adopt the multiple-scale method to represent the wave modulation and a boundary-layer scaling to incorporate the effects of viscosity and surfactant. For a water depth that is large in comparison with the length of the wave packet, a slow modulation in the vertical direction must be added, as introduced by McGoldrick (1970) and explained further by Mei (1983). The free-surface boundary layer has been considered in several studies of the mean drift in water waves, each in terms of coordinates such that a boundary-layer variable could be measured from the actual location of the free surface. Longuet-Higgins (1953) and Liu & Davis (1977) used a local curvilinear coordinate system moving with the free surface, Phillips (1966) and Craik (1982) chose a conformal transformation, and Ünlüata & Mei (1970) introduced a Lagrangian system.

In the present study, our goal is somewhat different, and the analysis is extended to higher order. One choice of coordinates that we considered initially was an orthogonal system obtained from a higher-order conformal transformation. It appeared to us, however, that a more straightforward formulation can be achieved by a nonorthogonal system with one coordinate measured horizontally and the other measured vertically from the exact location of the free surface.

The formulation for two-dimensional capillary-gravity waves is developed in §2, where the coordinate system and governing equations are presented. Suitable variables for the methods of multiple scales and matched asymptotic expansions are introduced, and the first-order inner and outer solutions are derived. In §3, a dissipative NLS equation is derived for viscous gravity waves with slowly varying amplitude. A solution for infinite wavetrains (the viscous equivalent of Stokes waves) is obtained, and the resulting damping coefficient is determined. In §4, capillary effects are added. The resulting dissipative NLS equation describes the effect of surfactants on the evolution of weakly nonlinear waves. Nonuniformities associated with the second- and the third-harmonic resonances and with pure capillary waves are discussed. Effects of viscosity and surfactants on the stability of weakly nonlinear waves are analyzed in §5. Numerical solutions to the dissipative NLS equations are obtained in §6; these solutions show the large-time modulation of viscous gravity and capillary-gravity waves in the presence of surfactants.

2 Formulation

We consider the slow evolution of two-dimensional surface waves influenced by an insoluble surfactant as well as by dispersion and weak nonlinearity. The extent of the wave packet is taken to be small in comparison with the fluid depth, so that the depth may be regarded as infinite. The fluid below the free surface has constant density ρ and viscosity μ, and the air above the free surface will be ignored. The surfactant is characterized by a surface dilational modulus M, which measures the resistance to the compression/expansion type of surface deformation (Lucassen, 1982). Changes in surfactant concentration cause the surface tension σ to vary in time and

space. The flow is caused by initial surface disturbances with small but finite amplitude, and is irrotational everywhere except in the boundary layer beneath the free surface, since the viscosity is considered to be small.

In general, the boundary-layer thickness may be much smaller than the wave amplitude. Since the boundary-layer part of the solution is expressed in terms of an inner variable measured from the surface, matching with an outer potential-flow solution is facilitated by the introduction of a coordinate system that moves with the free surface. One such system is a nonorthogonal coordinate system (x, y) generated simply by subtracting the free-surface elevation η from the vertical coordinate of a Cartesian system (x', y'):

$$x = x', \qquad y = y' - \eta(x, t), \tag{1}$$

where $\eta(x, t) = \eta(x', t)$ and y is directed upward from the mean free surface. The two components of the momentum equation are obtained by applying (1) to the nondimensional Navier-Stokes equations expressed in the Cartesian coordinate system (x', y'):

$$u_t + uu_x + (v - \eta_t - u\eta_x)u_y = -p_x + \eta_x p_y + \epsilon\left[u_{xx} + (1 + \eta_x^2)u_{yy} - 2\eta_x u_{xy} - \eta_{xx} u_y\right] \tag{2}$$

$$v_t + uv_x + (v - \eta_t - u\eta_x)v_y = -p_y + \epsilon\left[v_{xx} + (1 + \eta_x^2)v_{yy} - 2\eta_x v_{xy} - \eta_{xx} v_y\right]. \tag{3}$$

Here, the reciprocals of the wavenumber k and the frequency ω_o of the linear fundamental wave are used as the length and time scales, respectively. The horizontal and vertical velocity components u and v are scaled by ω_o/k, and the pressure p (with the hydrostatic component subtracted) is scaled by $\rho\omega_o^2/k^2$. Since the velocity vector is still written using the base vectors of the Cartesian coordinate system (x', y'), only the chain rule has been used to derive (2)-(3). The reciprocal of the Reynolds number, which is the primary small parameter, is defined as

$$\epsilon = \frac{k^2\mu}{\rho\omega_o}.$$

¿From the continuity equation for constant density, we have

$$u_x - \eta_x u_y + v_y = 0. \tag{4}$$

If the elements of the nondimensional stress tensor referred to the (x', y') coordinate system are denoted by τ_{ij}, and n_1 and n_2 are the x' and y' components of the unit vector normal to the surface, the surface force per unit area has x' and y' components F_1 and F_2 given by $F_i = \tau_{ij} n_j$. Since the slope of the free surface is η_x, the components of the outward normal are $n_1 = -\eta_x / L$ and $n_2 = 1/L$, where

$$L = (1 + \eta_x^2)^{1/2}.$$

The normal and tangential stresses then become $F_i n_i$ and $F_i t_i$, where $t_1 = n_2$ and $t_2 = -n_1$.

The normal stress on the free surface should balance the product of the curvature and the surface-tension coefficient when the pressure above the free surface is taken to be zero. In the present coordinate system, this condition is expressed as

$$p = \frac{2\epsilon}{L^2} \left[\eta_x^2 (u_x - \eta_x u_y) - \eta_x (u_y + v_x) + (1 + \eta_x^2) v_y \right] + G\eta - \frac{T}{L^3} \eta_{xx} \quad \text{at} \quad y = 0, \qquad (5)$$

where

$$G = \frac{kg}{\omega_o^2} \quad \text{and} \quad T = \frac{k^3 \sigma_o}{\rho \omega_o^2}$$

are the reciprocal of the Froude number and the Weber number, respectively. Here, g is the gravitational acceleration acting vertically downward, and σ_o is the undisturbed value of the surface tension. The boundary condition (5) is applied at the exact location of the free surface $y = 0$ due to the transformation (1).

The tangential stress on the free surface balances the surface-tension gradient σ_s, which can be related to the surface strain. If the displacement of a material point on the surface has x' and y' components ζ and η, the displacement component in a direction along the surface is $\zeta t_1 + \eta t_2$. The surface strain equals the derivative of the displacement with respect to distance s along the surface, and the gradient of surface tension is assumed to be proportional to the derivative of the strain. This gives a nonlinear extension of the insoluble-surfactant model used by Levich (1962), Lucassen-Reynders & Lucassen (1969), and others:

$$\sigma_s = \frac{M}{\epsilon} (\zeta + \eta \eta_x)_{ss},$$

where the surface dilational modulus M (or inverse surface compressibility) measures the change in surface tension resulting from a unit fractional area change. A complete rheological interpretation of this quantity was given by Lucassen-Reynders & Lucassen (1969). The nondimensional parameter $k^3M/(\rho\omega_o^2)$ is small and is chosen to be $O(\epsilon^{1/2})$ so that the effect of surfactants will appear in the first approximation to the boundary-layer solution (later in this section). A nondimensional surface dilational modulus is defined as

$$\kappa = \frac{k^3 M}{\rho\omega_o^2 \epsilon^{1/2}}.$$

In the present coordinate system, the required surface shear stress is then

$$2\eta_x (v_y - u_x + \eta_x u_y) + (1 - \eta_x^2)(u_y + v_x - \eta_x v_y) = \epsilon^{-1/2}\kappa(\zeta + \eta\eta_x)_{xx} \qquad \text{at} \quad y = 0. \tag{6}$$

Since both the horizontal and the vertical displacements of the free surface are introduced, two kinematic conditions on the free surface are needed to complete the governing equations:

$$v = \eta_t + u\eta_x \qquad \text{at} \quad y = 0 \tag{7}$$

$$u = \zeta_t + u\zeta_x \qquad \text{at} \quad y = 0. \tag{8}$$

Since we consider weak nonlinearity, we also require the initial amplitude a of the fundamental mode to be small. The relative importance of nonlinearity, surfactant, and viscosity is determined through the scaling of a, κ, and ϵ, respectively. Here, we choose κ to be $O(1)$ to observe the effect of surfactants in the first approximation. The relationship between a and the boundary-layer thickness, which is $O(\epsilon^{1/2})$, is chosen such that an amplitude equation with viscous effects can be determined at third order.

We introduce the slow variables

$$\tau = a^2 t, \quad \xi = a(x - c_g t), \quad \bar{y} = ay, \tag{9}$$

where c_g denotes the group velocity of the primary progressive wave. The first two small scales are identical to those used by Davey & Stewartson (1974) and Djordjevic & Redekopp (1977) for an

inviscid fluid with finite depth. The slow modulation in the vertical direction is added to suppress the inconsistency in the third-order solutions for infinite depth, as explained by Mei (1983) for an inviscid fluid. The slow variation in the horizontal direction thus requires a corresponding long-scale variation in the vertical direction, and the nondimensional depth is taken to be much larger than the extent of the wave packet, which is $O(a^{-1})$.

The flow outside the boundary layer can be described by a velocity potential ϕ, which should satisfy the Laplace equation. In the present coordinate system,

$$\phi_{xx} + \phi_{yy} = 2\eta_x\phi_{xy} + \eta_{xx}\phi_y - \eta_x^2\phi_{yy}. \tag{10}$$

We expand the velocity potential ϕ for small amplitude a:

$$\phi = a\phi_1 + a^2\phi_2 + a^3\phi_3 + \cdots. \tag{11}$$

By introducing the slow variables (9) and substituting the expansion (11) into (10), we then obtain, for increasing powers of a,

$$\phi_{1xx} + \phi_{1yy} = 0, \tag{12}$$

$$\phi_{2xx} + \phi_{2yy} = 2\eta_{1x}\phi_{1xy} + \eta_{1xx}\phi_{1y} - 2\phi_{1x\xi} - 2\phi_{1y\tilde{y}}, \tag{13}$$

$$\begin{aligned}\phi_{3xx} + \phi_{3yy} \;=\; & 2\eta_{1x}(\phi_{2xy} + \phi_{1x\tilde{y}} + \phi_{1\xi y}) + 2(\eta_{2x} + \eta_{1\xi})\phi_{1xy} + \phi_{1y}(\eta_{2xx} + 2\eta_{1x\xi}) \\ & + \eta_{1xx}(\phi_{1\tilde{y}} + \phi_{2y}) - 2\phi_{2x\xi} - \phi_{1\xi\xi} - 2\phi_{2y\tilde{y}} - \phi_{1\tilde{y}\tilde{y}} - \eta_{1x}^2\phi_{1yy}.\end{aligned} \tag{14}$$

The lowest-order equation (12) gives

$$\phi_1 = (AE + A^cE^{-1})e^y, \tag{15}$$

where

$$E \equiv \exp\{i(x - t)\} \tag{16}$$

and $A(\xi, \tau)$ describes a slow variation of amplitude with a mean value of $\frac{1}{2}$ at $\tau = 0$, since a is the initial amplitude of this mode. The superscript c denotes the complex conjugate, and i is $\sqrt{-1}$. Since the factor e^y in (15) decays exponentially with depth, the slowly varying amplitude

A need not depend on $\bar{y}$. In general, a long-scale velocity potential $\phi_1^0(\xi, \bar{y}, \tau)$ can be added to the right-hand-side of (15), which should satisfy $\phi^0_{1\xi\xi} + \phi^0_{1\bar{y}\bar{y}} = 0$ to avoid secular terms arising from (14). Also, the boundary condition $\phi^0_{1\bar{y}}(\bar{y} = 0) = 0$ should be imposed to suppress secular terms in the second-order free-surface elevation η_2 below. In the present study, we set $\phi_1^0 = 0$. An example of nonzero ϕ_1^0 for a time-varying current is given by Mei (1983).

The velocity components are obtained from the gradient of the velocity potential (11) in the x' and y' coordinates with the transformation (1):

$$u = ai(AE - A^cE^{-1})e^y + a^2(\phi_{2x} + \phi_{1\xi} - \eta_{1x}\phi_{1y}) + \cdots \tag{17}$$

$$v = a(AE + A^cE^{-1})e^y + a^2\phi_{2y} + a^3(\phi_{3y} + \phi_{2\bar{y}}) + \cdots. \tag{18}$$

¿From the Bernoulli equation, the pressure for the outer region of irrotational flow is

$$p = ai(AE - A^cE^{-1})e^y - a^2[\phi_{2t} - c_g\phi_{1\xi} - \eta_{1t}\phi_{1y} + \frac{1}{2}(\phi_{1x}^2 + \phi_{1y}^2)] - a^3[\phi_{3t} - c_g\phi_{2\xi} + \phi_{1\tau}$$
$$-\eta_{1t}\phi_{2y} + (\phi_{2y} - \eta_{2t} + c_g\eta_{1\xi})\phi_{1y} + (\phi_{2x} + \phi_{1\xi})\phi_{1x} - \eta_{1x}\phi_{1x}\phi_{1y}] + \cdots. \tag{19}$$

In the boundary layer, the system (2)-(8) is solved after introducing the slow variables (9) and the inner coordinate

$$y^* = \frac{y}{\sqrt{\epsilon}}. \tag{20}$$

Velocity components, pressure, and free-surface displacements are expanded for large Reynolds number. The gauge functions for the inner expansions are to be determined after the scale of the amplitude is chosen. Independent of the scale, the first-order boundary-layer equations become, in the order of usage:

$$v^*_{1y^*} = 0 \tag{21}$$

$$\eta_{1t} = v_1^* \quad \text{at} \quad y^* = 0 \tag{22}$$

$$p^*_{1y^*} = 0 \tag{23}$$

$$p_1^* = G\eta_1 - T\eta_{1xx} \quad \text{at} \quad y^* = 0 \tag{24}$$

$$u^*_{1y^*y^*} - u^*_{1t} = p^*_{1x} \tag{25}$$

$$u^*_{1y^*t} = \kappa u^*_{1xx} \quad \text{at} \quad y^* = 0 \tag{26}$$

$$\zeta_{1t} = u^*_1 \quad \text{at} \quad y^* = 0, \tag{27}$$

where u^*_1, v^*_1, and p^*_1 are the first-order inner solutions. The boundary condition for u^*_1 in (26) is obtained by differentiating (6) with respect to time and applying (8). The solutions must also match with the outer solutions (17)-(19). After matching conditions are applied, the solutions become

$$v^*_1 = AE + c.c. \tag{28}$$

$$\eta_1 = iAE + c.c \tag{29}$$

$$p^*_1 = iAE + c.c. \tag{30}$$

$$u^*_1 = (Q_1 + i)AE + c.c. \tag{31}$$

$$\zeta_1 = (iQ_0 - 1)AE + c.c. \ , \tag{32}$$

where

$$Q_1 = \frac{\sqrt{2}\kappa}{1 - i(1 - \sqrt{2}\kappa)} \exp\left(\frac{1-i}{\sqrt{2}} y^*\right) \equiv Q_0 \exp\left(\frac{1-i}{\sqrt{2}} y^*\right),$$

and $c.c.$ denotes the complex conjugate. The linear dispersion equation

$$G + T = 1 \tag{33}$$

is obtained from the boundary and matching conditions for the pressure and is not affected by surfactants.

The development of the solutions to (2)-(8) beginning with the outer solution for ϕ_2 is now straightforward. The matching condition for the second-order pressure gives the group velocity c_g. At third order, where we terminate the analysis, the matching condition yields an evolution equation for $A(\xi, \tau)$ in the form of a dissipative NLS equation that includes the effects of viscosity, surface tension, and surfactant. This dissipative NLS equation can be used to obtain the damping coefficient and to examine the stability of weakly nonlinear waves.

3 Gravity wave

We first examine the case when the capillary effect is absent; i.e., we take $T = 0$ and then, by necessity, $\kappa = 0$. The wave amplitude is chosen to be of the same order as the boundary-layer thickness, so that

$$\lambda a = \epsilon^{1/2}, \tag{34}$$

where $\lambda = O(1)$ is a proportionality constant. The gauge functions for the inner expansions should then be

$$\delta_i(\epsilon) = \left(\frac{\epsilon^{1/2}}{\lambda}\right)^i, \tag{35}$$

where λ is inserted for convenience. We have verified at each step that this is the correct sequence for the first few terms. The first-order inner and outer solutions are identical to those in the previous section except that G is replaced by unity, and Q_1 and Q_0 in (31) and (32) are absent; thus u_1^* is independent of y^*.

The second-order term, $O(\epsilon)$, in the potential is found from (13),

$$\phi_{2xx} + \phi_{2yy} = -3iA^2E^2e^{y} - 2iA_\xi Ee^{y} + c.c. \ , \tag{36}$$

and we set

$$\phi_2 = iA^2E^2e^{y} - iA_\xi Eye^{y} + c.c. + \phi_2^0(\xi, \bar{y}, \tau). \tag{37}$$

The solution to the homogeneous equation, $F_2(\xi, \bar{y}, \tau)E^2e^{2y} + F_1(\xi, \bar{y}, \tau)Ee^{y} + c.c.$, is not included. Matching shows that $F_2 = 0$. The other coefficient F_1 remains arbitrary and may be set to zero; taking $F_1 \neq 0$ would be equivalent to changing A by an amount aF_1. The long-scale velocity potential ϕ_2^0 should satisfy

$$\phi^0_{2\xi\xi} + \phi^0_{2\bar{y}\bar{y}} = 0, \tag{38}$$

which can be obtained by extending the expansions (12)-(14) to the fourth order. (From another viewpoint, the flow at large distances such that $\xi = O(1)$ and $\bar{y} = O(1)$ is described by (38).) The boundary condition for ϕ_2^0 will be determined at third order. The second-order velocity

components and the pressure in the outer region, from (17)-(19), become

$$u_2 = A_\xi E(e^y + ye^y) - A^2E^2e^y + c.c. + 2\,|A|^2\,e^y \tag{39}$$

$$v_2 = iA^2E^2e^y - iA_\xi E(e^y + ye^y) + c.c. \tag{40}$$

$$p_2 = -A^2E^2e^y + A_\xi E(c_g e^y + ye^y) + c.c. + 2\,|A|^2\,(e^y - e^{2y}). \tag{41}$$

In the boundary layer, the second-order equations are

$$\frac{1}{\lambda}v^*_{2y^*} = -u^*_{1x} \tag{42}$$

$$\eta_{2t} = v^*_2 - u^*_1\eta_{1x} + c_g\eta_{1\xi} \quad \text{at} \quad y^* = 0 \tag{43}$$

$$\frac{1}{\lambda}p^*_{2y^*} = -v^*_{1t} \tag{44}$$

$$p^*_2 = \eta_2 \quad \text{at} \quad y^* = 0 \tag{45}$$

$$u^*_{2y^*y^*} - u^*_{2t} = p^*_{2x} - \frac{1}{\lambda}\eta_{1x}p^*_{2y^*} + p^*_{1\xi} - c_g u^*_{1\xi} + u^*_1 u^*_{1x} \tag{46}$$

$$\frac{1}{\lambda}u^*_{2y^*} = -v^*_{1x} \quad \text{at} \quad y^* = 0. \tag{47}$$

After matching with the outer solutions, the solutions to (42)-(47) become

$$v^*_2 = \lambda AEy^* + iA^2E^2 - iA_\xi E + c.c. \tag{48}$$

$$\eta_2 = -A^2E^2 + \frac{1}{2}A_\xi E + c.c. \tag{49}$$

$$p^*_2 = i\lambda AEy^* - A^2E^2 + \frac{1}{2}A_\xi E + c.c. \tag{50}$$

$$u^*_2 = \lambda\sqrt{2}(1-i)\exp\left(\frac{1-i}{\sqrt{2}}y^*\right)AE + i\lambda AEy^* - A^2E^2 + A_\xi E + c.c. + 2\,|A|^2\,. \tag{51}$$

A long-scale free-surface elevation $\eta^0_2(\xi,\tau)$ that could appear in (49) as a result of integrating (43) has been set to zero as a consequence of matching the pressure. Also, the group velocity c_g has been replaced by $\frac{1}{2}$.

The third-order outer solutions, $O(\epsilon^{3/2})$, are obtained first by solving

$$\begin{aligned}\phi_{3xx} + \phi_{3yy} \;=\; & 12A^3E^3e^y - AA_\xi E^2(\frac{5}{2}e^y + 3ye^y) \\ & -AA^\xi_\xi(\frac{5}{2}e^y + ye^y) - A_{\xi\xi}E(e^y + 2ye^y) + c.c.\end{aligned} \tag{52}$$

The solution to the homogeneous equation is dropped for the same reason as cited for ϕ_2 in (37). We try a solution for (52) of the form

$$\phi_3 = -\frac{3}{2}A^3E^3e^y + AA_\xi E^2(\frac{3}{2}e^y + ye^y) - AA^c_\xi(\frac{1}{2}e^y + ye^y) - \frac{1}{2}A_{\xi\xi}Ey^2e^y + c.c. + \phi^0_3(\xi, \bar{y}, \tau). \quad (53)$$

The outer solutions for the vertical component of the velocity and the hydrodynamic pressure are then obtained from (18)-(19):

$$\begin{aligned} v_3 &= -\frac{3}{2}A^3E^3e^y + AA_\xi E^2(\frac{5}{2}e^y + ye^y) - AA^c_\xi(\frac{3}{2}e^y + ye^y) \\ &\quad -\frac{1}{2}A_{\xi\xi}E(2+y)ye^y + c.c. + \phi^0_{2g} \end{aligned} \quad (54)$$

$$\begin{aligned} p_3 &= -i\frac{3}{2}A^3E^3e^y + iAA^c_\xi(e^y - e^{2y} - ye^{2y}) - \frac{i}{2}A_{\xi\xi}E(1+y)ye^y \\ &\quad -A_\tau Ee^y + i\,|A|^2\,AE(3e^y - 4e^{2y}) + iAA_\xi E^2(e^y + e^{2y} + ye^{2y}) + c.c. + \frac{1}{2}\phi^0_{2\xi}. \end{aligned} \quad (55)$$

The boundary-layer equations at third order are

$$\frac{1}{\lambda}v^*_{3y^*} = \frac{1}{\lambda}\eta_{1x}u^*_{2y^*} - u^*_{2x} - u^*_{1\xi} \quad (56)$$

$$\eta_{3t} = v^*_3 + \frac{1}{2}\eta_{2\xi} - \eta_{1\tau} - u^*_1(\eta_{2x} + \eta_{1\xi}) - u^*_2\eta_{1x} \qquad at \quad y^* = 0 \quad (57)$$

$$\frac{1}{\lambda}p^*_{3y^*} = -v^*_{2t} + \frac{1}{2}v^*_{1\xi} - u^*_1v^*_{1x} \quad (58)$$

$$p^*_3 = 2\lambda v^*_{2y^*} + \eta_3 \qquad at \quad y^* = 0. \quad (59)$$

The equations for u^*_3 are omitted since they are not required for derivation of the desired amplitude equation. After matching with (18), equation (56) gives

$$\begin{aligned} v^*_3 &= -\lambda\sqrt{2}(1-i)\exp\left(\frac{1-i}{\sqrt{2}}y^*\right)\left(A^2E^2 - \frac{1-i}{\sqrt{2}}\lambda AE + |A|^2\right) + \lambda iA^2E^2y^* \\ &\quad +\lambda^2\frac{1}{2}AEy^{*2} - 2i\lambda A_\xi Ey^* - \frac{3}{2}A^3E^3 + \frac{5}{2}AA_\xi E^2 - \frac{3}{2}AA^c_\xi + c.c. + \phi^0_{2g}. \end{aligned} \quad (60)$$

Integrating (57) then yields the third-order free-surface elevation:

$$\eta_3 = -\frac{3}{2}iA^3E^3 + 3i\,|A|^2\,AE + 2\lambda^2AE + 2iAA_\xi E^2 + \frac{i}{4}A_{\xi\xi}E + A_\tau E + c.c. + \eta^0_3(\xi, \tau), \quad (61)$$

where the condition

$$\phi^0_{2\bar{y}} = 2\frac{\partial \mid A \mid^2}{\partial \xi} \qquad \text{at} \quad \bar{y} = 0 \tag{62}$$

has been imposed to suppress secular terms. The equation for p^*_3 with the boundary condition (59) can easily be solved to yield

$$\begin{aligned} p^*_3 \;=\; & \frac{i}{2}\lambda^2 A E y^{*2} - \lambda A^2 E^2 y^* + \frac{3}{2}\lambda A_\xi E y^* + 4\lambda^2 A E - \frac{3}{2} i A^3 E^3 + 3i \mid A \mid^2 A E \\ & 2iAA_\xi E^2 + \frac{i}{4} A_{\xi\xi} E + A_\tau E + c.c. - 2\lambda \mid A \mid^2 y^* + \eta^0_3(\xi, \tau). \end{aligned} \tag{63}$$

The matching condition for the third-order pressure (63) with the outer solution (19) finally gives

$$\eta^0_3(\xi, \tau) = \frac{1}{2}\phi^0_{2\xi} \qquad \text{at} \quad \bar{y} = 0, \tag{64}$$

for terms independent of E, and

$$iA_\tau + 2i\lambda^2 A - \frac{1}{8} A_{\xi\xi} = 2 \mid A \mid^2 A, \tag{65}$$

for terms linear in E.

Except for an additional term $2i\lambda^2 A$, the amplitude equation (65) is identical to the NLS equation that governs the amplitude modulation of gravity waves in inviscid flow. It is thus appropriate to call the amplitude equation a dissipative NLS equation. ¿From (65), the integral of $\mid A \mid^2$ over ξ is easily found to decay as $\exp(-4\lambda^2 \tau)$.

For infinite wavetrains independent of ξ, the solution $A_0(\tau)$ of (65) that satisfies $A_0(0) = a_0$ is

$$A_0(\tau) = a_0 \exp\left[-2\lambda^2 \tau + \frac{i}{2\lambda^2} \mid a_0 \mid^2 (e^{-4\lambda^2 \tau} - 1)\right], \tag{66}$$

where a_0 is a complex constant with $\mid a_0 \mid = 1/2$, as explained earlier. Here, the expression $\mid a_0 \mid^2$ is kept to show the amplitude dependence explicitly. In the inviscid limit, $\lambda \to 0$, the Stokes wave (to third order) is recovered:

$$A_0(\tau) = a_0 \exp\left(-2i \mid a_0 \mid^2 \tau\right). \tag{67}$$

The decaying factor in (66), combined with (9) and (34), becomes $\exp(-2\epsilon t)$. Thus, the damping coefficient D_g for weakly nonlinear gravity waves is

$$D_g = 2\epsilon, \tag{68}$$

which is identical to the linear result of Stokes (1845). In retrospect, we could instead have shown that the damping coefficient is unaffected by nonlinearity at this order using the dissipation function and its expansion for small amplitude. Viscosity also causes a phase shift, as can be seen from (66). Although viscous dissipation causes exponential decay in the amplitude of nonlinear waves, it is not clear whether it can suppress a modulational instability of the Benjamin-Feir type and the subsequent recurrence phenomenon. We will examine this in §5.

4 Capillary-gravity waves

We now consider capillary-gravity waves with a surfactant on the free surface. For the gravity wave in the previous section, the amplitude of the wave is chosen to be of the same order as the boundary-layer thickness so that nonlinearity and dissipation both appear in the amplitude equation. When a surfactant is present, however, lower-order dissipation is expected; thus, the amplitude is chosen to be of lower order than the boundary-layer thickness:

$$\lambda a = \epsilon^{1/4}, \tag{69}$$

where λ is again a proportionality constant. The gauge functions for the inner expansions now become

$$\delta_i(\epsilon) = \left(\frac{\epsilon^{1/4}}{\lambda}\right)^i. \tag{70}$$

The first-order solutions, $O(\epsilon^{1/4})$, are as given by (17)-(19) for the outer region of irrotational flow and by (28)-(32) for the boundary layer. Since the nondimensional surface dilational modulus κ and the Weber number T are nonzero, the boundary-layer solutions for the horizontal velocity component (31) and displacement (32) are affected by the surfactant at the leading order, and the linear dispersion relationship (33) is that for capillary-gravity waves.

The equation for the $O(\epsilon^{1/2})$ term ϕ_2 in the velocity potential is identical to (36), but the appropriate solution now includes a solution of the homogeneous equation:

$$\phi_2 = FE^2e^{2y} + iA^2E^2e^y - iA_\xi Eye^y + c.c. + \phi_2^0(\xi, \bar{y}, \tau), \tag{71}$$

where $F(\xi, \tau)$ can be determined through a matching condition. Again, the long-scale potential ϕ_2^0 should satisfy the Laplace equation (38), with the boundary condition to be determined through matching of the third-order solutions. The velocity components and the pressure in the outer region, from (17)-(19), then become

$$u_2 = 2iFE^2e^{2y} + A_\xi E(e^y + ye^y) - A^2E^2e^y + c.c. + 2\,|A|^2\,e^y \tag{72}$$

$$v_2 = 2FE^2e^{2y} + iA^2E^2e^y - iA_\xi E(e^y + ye^y) + c.c. \tag{73}$$

$$p_2 = 2iFE^2e^{2y} - A^2E^2e^y + A_\xi E(c_g e^y + ye^y) + c.c. + 2\,|A|^2\,(e^y - e^{2y}). \tag{74}$$

The boundary-layer equations for the $O(\epsilon^{1/2})$ terms differ from those for the gravity wave in the previous section because the amplitude considered here is of lower order than the boundary-layer thickness. Substituting the inner expansions into (2)-(8) and using the multiple scales (9), the inner variable (20), and the amplitude (69), we obtain

$$v^*_{2y^*} = \eta_{1x} u^*_{1y^*} \tag{75}$$

$$\eta_{2t} = v^*_2 - u^*_1\eta_{1x} + c_g\eta_{1\xi} \qquad \text{at} \quad y^* = 0 \tag{76}$$

$$p^*_{2y^*} = 0 \tag{77}$$

$$p^*_2 = G\eta_2 - T(\eta_{2xx} + 2\eta_{1x\xi}) \quad \text{at} \quad y^* = 0 \tag{78}$$

$$u^*_{2y^*y^*} - u^*_{2t} = p^*_{2x} + p^*_{1\xi} - \frac{1}{\lambda^2}\eta_{1x}p^*_{3y^*} + u^*_1u^*_{1x} - c_g u^*_{1\xi} \tag{79}$$

$$u^*_{2y^*} = \kappa\{(\zeta_2 + \eta_1\eta_{1x})_{xx} + 2\zeta_{1x\xi}\} \quad \text{at} \quad y^* = 0. \tag{80}$$

The third approximation to the y^* momentum equation is also needed, to eliminate $p^*_{3y^*}$ from (79):

$$\frac{1}{\lambda^2}p^*_{3y^*} = -v^*_{1t}. \tag{81}$$

The vertical velocity component v_2^* is obtained by integrating (75) and imposing the matching condition:

$$v_2^* = -Q_1 \mid A \mid^2 + 2FE^2 + (i - Q_1)A^2E^2 - iA_\xi E + c.c. \tag{82}$$

Then, from (76), the second-order free-surface elevation becomes

$$\eta_2 = iFE^2 - A^2E^2 + (1 - c_g)A_\xi E + c.c., \tag{83}$$

where the long-scale quantity $\eta_2^0(\xi, \bar{y}, \tau)$ is omitted in anticipation of the matching condition for the second-order pressure. After (83) is substituted into the boundary condition for p_2^* in (78), the inner solution for the second-order pressure is obtained:

$$p_2^* = (1 + 3T)(iF - A^2)E^2 + (1 - c_g + 2T)A_\xi E + c.c. \tag{84}$$

The solution (84) should match the outer solution (19), with the terms $O(\epsilon^{1/2})$ replaced by (74). Therefore, the slowly varying amplitude F and the group velocity c_g are obtained as

$$F = \frac{i3T}{1 - 3T}A^2 \tag{85}$$

$$c_g = \frac{1 + 2T}{2}, \tag{86}$$

respectively. The group velocity (86) agrees with the relationship for a linear capillary-gravity wave in inviscid flow. It is noteworthy that F blows up as $T \to 1/3$; thus, a second-harmonic resonance persists despite the effects of viscosity and surfactants. A complete discussion of this resonant behavior was given by McGoldrick (1970). A modified asymptotic flow description is needed for small values of $|T - 1/3|$ and will be discussed later in this section.

Substituting the known solutions into the right-hand side of the boundary-layer equation for u_2^* in (79) gives

$$u_{2y^*y^*}^* - u_{2t}^* = \left[iQ_1^2 - 2Q_1 - i\frac{2(1 + 3T)}{1 - 3T}\right] A^2E^2 + (i - c_gQ_1)A_\xi E + c.c. \tag{87}$$

The boundary condition for u_2^* in (79) can be applied more conveniently after it is differentiated with respect to time and the kinematic boundary condition (8) is introduced:

$$u_{2ty^*}^* - \kappa u_{2xx}^* = -4\kappa(Q_0^2 + 2iQ_0 - 3)A^2E^2 + \kappa(2 - c_g)(iQ_0 - 1)A_\xi E + c.c. \quad \text{at} \quad y^* = 0. \tag{88}$$

Then, from (87) and (88), the second-order horizontal velocity component is

$$u_2^* = \left[q_1 e^{(1-i)y^*} - \frac{1}{2}Q_1^2 + 2iQ_1\right] A^2E^2 + \left[q_2 \exp\left(\frac{1-i}{\sqrt{2}}y^*\right) + 1 - \frac{c_g}{\sqrt{2}(1-i)}y^*Q_1\right] A_\xi E$$
$$-\frac{1+3T}{1-3T}A^2E^2 + c.c + 2\,|A|^2, \tag{89}$$

where

$$q_1 = -\frac{1}{2\kappa - 1 - i}\left[\left(\frac{1+i}{\sqrt{2}} + \kappa\right)Q_0^2 + \{\sqrt{2} + i(8\kappa - \sqrt{2})\}Q_0 + 4\kappa\frac{2-3T}{1-3T}\right]$$

and

$$q_2 = \frac{\left[i2\sqrt{2}(2-c_g) + (1-i)c_g\right]Q_0 - 2\sqrt{2}(1-c_g)}{2(\sqrt{2}\,\kappa - 1 - i)}.$$

In the third approximation, $O(\epsilon^{3/4})$, the velocity potential ϕ_3 should satisfy (14), or

$$\phi_{3xx} + \phi_{3yy} = A^3E^3\left[\frac{30T}{1-3T}e^{2y} + \frac{12(1-T)}{1-3T}e^y\right] + |A|^2\,AE\frac{18T}{1-3T}e^{2y}$$
$$-A_{\xi\xi}E(e^y + 2ye^y) + AA_\xi E^2\left(\frac{6T-5}{2}e^y - 3ye^y + \frac{24T}{1-3T}e^{2y}\right)$$
$$-AA_\xi^c\left(\frac{5-2T}{2}e^y + ye^y\right) + c.c. \tag{90}$$

The appropriate solution of (90) is

$$\phi_3 = F_3E^3e^{3y} + F_2E^2e^{2y} - A^3E^3\left[\frac{3(1-T)}{2(1-3T)}e^y + \frac{6T}{1-3T}e^{2y}\right] + |A|^2\,AE\frac{6T}{1-3T}e^{2y}$$
$$+AA_\xi E^2\left(\frac{3-2T}{2}e^y + ye^y + \frac{6T}{1-3T}ye^{2y}\right) - AA_\xi^c\left(\frac{1-2T}{2}e^y + ye^y\right)$$
$$-\frac{1}{2}A_{\xi\xi}Ey^2e^y + c.c. + \phi_3^0(\xi, \bar{y}, \tau), \tag{91}$$

where the slowly varying amplitudes $F_3(\xi,\tau)$ and $F_2(\xi,\tau)$ are to be determined from the matching condition. As in the derivation of ϕ_2, a first-harmonic term in the solution to the homogeneous equation is dropped. The vertical velocity component v_3 is then obtained from (18) as

$$v_3 = 3F_3E^3e^{3y} + 2F_2E^2e^{2y} - A^3E^3\left[\frac{3(1-T)}{2(1-3T)}e^y + \frac{12T}{1-3T}e^{2y}\right] + |A|^2\,AE\frac{12T}{1-3T}e^{2y}$$
$$+AA_\xi E^2\left(\frac{5-2T}{2}e^y + ye^y + \frac{6T}{1-3T}e^{2y} + \frac{12T}{1-3T}ye^{2y}\right) - AA_\xi^c\left(\frac{3-2T}{2}e^y + ye^y\right)$$
$$-A_{\xi\xi}E\left(ye^y + \frac{y^2}{2}e^y\right) + c.c. + \phi_{2g}^0. \tag{92}$$

Replacing the $O(\epsilon^{3/4})$ terms in (19) with the known solutions yields

$$\begin{aligned} p_3 &= i3F_3E^3e^{3y} + i2F_2E^2e^{2y} - iA^3E^3\left[\frac{5-9T}{2(1-3T)}e^y - \frac{1-21T}{1-3T}e^{2y} - \frac{6T}{1-3T}e^{3y}\right] \\ &+iAA_\xi E^2\left[3e^y + 2ye^y - \frac{1-6T-6T^2}{1-3T}e^{2y} - \frac{1-15T}{1-3T}ye^{2y}\right] \\ &+i\,|A|^2\,AE\left[\frac{2}{1-3T}e^y - \frac{3(1-5T)}{1-3T}e^{2y} - \frac{6T}{1-3T}e^{3y}\right] - iA_{\xi\xi}E\left(\frac{y^2}{2}e^y + \frac{1+2T}{2}ye^y\right) \\ &+iAA_\xi^c(e^y - e^{2y} - ye^{2y}) - A_\tau Ee^y + c.c. + (\eta_{1t} - \phi_{1y})\phi_{2y} + c_g\phi_{2\xi}^0. \end{aligned} \tag{93}$$

The third-order boundary-layer solutions are again obtained from the continuity equation (4) for v_3^*, the free-surface boundary condition (7), and the vertical momentum equation (3) for p_3^*. The equation for the vertical velocity component then becomes

$$v_{3y^*}^* = -\lambda^2 u_{1x}^* + \eta_{1x}u_{2y^*}^* + \eta_{2x}u_{1y^*}^*, \tag{94}$$

which gives

$$\begin{aligned} v_3^* &= [(\frac{1-i}{\sqrt{2}}Q_1 + \lambda^2 y^*)AE + c.c] - \frac{2}{1-3T}(iA^2E^2 + c.c)(Q_1AE + c.c) - (AE + c.c)\cdot \\ &\cdot\left[(q_1e^{(1-i)y^*} - \frac{1}{2}Q_1^2 + 2iQ_1)A^2E^2 + \{q_2\exp\left(\frac{1-i}{\sqrt{2}}y^*\right) - \frac{c_g}{\sqrt{2}(1-i)}y^*Q_1\}A_\xi E + c.c\right] \\ &+\left[3\{F_3 - \frac{1+7T}{2(1-3T)}A^3\}E^3 + 2F_2E^2 + c.c\right] + \frac{1-2T}{2}(iA_\xi E + c.c)(Q_1AE + c.c) \\ &+\left[\frac{12T}{1-3T}\,|A|^2\,AE - \frac{3-2T}{2}AA_\xi^c + \frac{6T^2-5T+5}{2(1-3T)}AA_\xi E^2 + c.c\right] + \phi_{2g}^0, \end{aligned} \tag{95}$$

after the matching condition is applied. The third-order free-surface elevation η_3 is obtained by integrating

$$\eta_{3t} = v_3^* + c_g\eta_{2\xi} - \eta_{1\tau} - u_1^*(\eta_{2x} + \eta_{1\xi}) - u_2^*\eta_{1x} \quad \text{at} \quad y^* = 0. \tag{96}$$

The result after appropriate substitutions is

$$\begin{aligned} \eta_3 &= i\left[F_3 - \frac{3(1+3T)}{2(1-3T)}A^3\right]E^3 + \left[iF_2 + \{i\frac{6T^2-13T+4}{2(1-3T)} + \frac{1}{2}Q_0\}AA_\xi\right]E^2 \\ &+\frac{3(1+T)}{1-3T}i\,|A|^2\,AE + (\frac{1}{4} - T^2)iA_{\xi\xi}E + A_\tau E + \frac{1+i}{\sqrt{2}}Q_0AE + c.c. + \eta_3^0 \end{aligned} \tag{97}$$

where the condition

$$\phi_{2g}^0 = 2(1-T)\,|A^2|_\xi - i(Q_0AA_\xi^c - Q_0^cA^cA_\xi) \qquad \text{at} \quad \bar{y} = 0 \tag{98}$$

has been imposed to suppress secular terms. As mentioned earlier, (98) is the boundary condition for ϕ_2^0; thus, ϕ_2^0 is uniquely determined once A is obtained from (104) below. It is noteworthy that additional nonlinear forcing terms are present in (98) because of the surfactant.

The differential equation for p_3^* is (81), and the associated boundary condition is

$$p_3^* = 2\lambda^2 v_{1y}^* + G\eta_3 - T(\eta_{3xx} + 2\eta_{2x\xi} + \eta_{1\xi\xi}) + \frac{3}{2}T\eta_{1x}^2\eta_{1xx}. \tag{99}$$

Solving (81) subject to (99) results in

$$\begin{aligned} p_3^* &= i\left[(1+8T)F_3 - \frac{3(1+12T+21T^2)}{2(1-3T)}A^3\right]E^3 + i(1+3T)F_2E^2 \\ &+ \left[i\frac{(1+3T)(4-13T+6T^2)+16T}{2(1-3T)} + \frac{1+3T}{2}Q_0\right]AA_\xi E^2 + \lambda^2(iy^* + \frac{1+i}{\sqrt{2}}Q_0)AE \\ &+ i\frac{1-8T+4T^2}{4}A_{\xi\xi}E + A_\tau E + i\frac{6+3T+9T^2}{2(1-3T)}|A|^2AE + c.c. + G\eta_3^0. \end{aligned} \tag{100}$$

Applying the matching condition for the pressure, we determine F_2 and F_3:

$$F_3 = -\frac{3T(5+21T)}{4(1-3T)(1-4T)}A^3, \tag{101}$$

$$F_2 = \left[\frac{3T(7-15T+6T^2)}{2(1-3T)^2} - i\frac{1+3T}{2(1-3T)}Q_0\right]AA_\xi. \tag{102}$$

We also obtain

$$\eta_3^0 = \frac{1+2T}{2(1-T)}\phi_{2\xi}^0 \tag{103}$$

and the amplitude equation for the capillary-gravity wave with viscosity and surfactant:

$$iA_\tau + \frac{i\lambda^2}{2\sqrt{2}}\cdot\frac{\kappa[\kappa+i(\sqrt{2}-\kappa)]}{\kappa^2-\sqrt{2}\kappa+1}A - \frac{1}{8}(4T^2-8T+1)A_{\xi\xi} = \frac{9T^2-15T+8}{4(1-3T)}|A|^2A. \tag{104}$$

Two more nonuniformities are observed, in addition to the one for the second-harmonic resonance ($T = 1/3$). In (101), the amplitude F_3 becomes unbounded as T approaches 1/4; thus, a third-harmonic resonance occurs. As T approaches unity (the value for pure capillary waves), η_3^0 in (103) is singular, and a rescaling of the long-scale free-surface elevations is required, as explained below.

The dissipation term proportional to A in (104) is attributed to the surfactant, whereas for a clean surface the dissipation is of higher order, as shown in the previous section where different scaling was required. Therefore, if either λ or κ is zero, the dissipation term in (104) is absent, and we recover the amplitude equation for capillary-gravity waves in inviscid flow. In these cases, the resulting NLS equation could also be obtained more easily in a Cartesian coordinate system by incorporating the vertical modulation $\bar{y}$ in the derivation of Djordjevic & Redekopp (1977) for finite depth. In the dissipative NLS equation (104), the linear dissipation term has a complex coefficient; the imaginary part is related to the decay rate, and the real part corresponds to a frequency change due to the surfactant.

A solution of (104) for infinite wavetrains which depends only on τ is

$$A_0 = a_0 \exp\left[-\frac{\lambda^2}{2\sqrt{2}}\frac{\kappa^2+i(\sqrt{2}\kappa-\kappa^2)}{\kappa^2-\sqrt{2}\kappa+1}\tau\right]\cdot\exp\left[i\,|a_0|^2\left(\frac{9T^2-15T+8}{1-3T}\right)\cdot\left(\frac{\kappa^2-\sqrt{2}\kappa+1}{2\sqrt{2}\kappa^2\lambda^2}\right)\left\{\exp\left(-\frac{1}{\sqrt{2}}\frac{\kappa^2\lambda^2}{\kappa^2-\sqrt{2}\kappa+1}\tau\right)-1\right\}\right]. \tag{105}$$

Since the slow time is now defined as $\tau = \epsilon^{1/2}t/\lambda^2$ due to (69), the damping coefficient D_s for an infinite wavetrain (105) becomes

$$D_s = \frac{\sqrt{2}\kappa^2}{4(\kappa^2-\sqrt{2}\kappa+1)}\epsilon^{1/2}, \tag{106}$$

which has a maximum at $\kappa = \sqrt{2}$. At this maximum, the frequency shift due to the surfactant disappears. The damping coefficient (106) agrees with the results of Levich (1941, 1972) and Lucassen-Reynders & Lucassen (1969) for linear capillary waves, as can be seen by expanding their solutions for large Reynolds number. It is clear from the result that the damping effect is greatly enhanced by the surfactant.

In the derivation of these expansions, we have noted that singular behavior appears for certain values of the Weber number. The case for $T = 1/3$ corresponds to second-harmonic resonance and is related to Wilton's ripples. The nonuniformity can be removed by considering a superposition of the fundamental wave and its second harmonic in the first approximation and by adding an intermediate slow time scale, as in McGoldrick (1970) for inviscid flow. We start by considering

a Weber number near the value for the resonance:

$$T = \frac{1}{3} + a\tilde{T}, \tag{107}$$

where $\tilde{T} = O(1)$ is a constant. An appropriate solution for (12) is now

$$\phi_1 = A_1(\xi, \tilde{t})Ee^y + A_2(\xi, \tilde{t})E^2e^{2y} + c.c., \tag{108}$$

instead of (15), where

$$\tilde{t} = at = \tau/a \tag{109}$$

is the new time variable. The subsequent analysis proceeds as before except for the added complexity due to the presence of second-harmonic terms in the first-order solutions. For example, an equation analogous to (36) is

$$\begin{aligned} \phi_{2xx} + \phi_{2yy} &= -24iA_2^2E^4e^{2y} - iA_1A_2E^3\left(10e^{2y} + 8e^y\right) - 3iA_1^2E^2e^y \\ &\quad -6iA_1^cA_2Ee^{2y} - 2iA_{1\xi}Ee^y - 4iA_{2\xi}Ee^{2y} + c.c., \end{aligned} \tag{110}$$

and an appropriate solution of the homogeneous equation should include third- and fourth-harmonic terms. A matching condition for the second-order pressure finally gives

$$A_{1\tilde{t}} = -A_1^cA_2 \tag{111}$$

$$A_{2\tilde{t}} + i\frac{3\tilde{T}}{2}A_2 + \frac{1}{3}A_{2\xi} = \frac{1}{2}A_1^2, \tag{112}$$

in addition to the group velocity $c_g = 5/6$, the correct value when $T = 1/3$.

The evolution equations (111)-(112) are equivalent to the second-harmonic resonance equations given by McGoldrick (1970), except that a term proportional to $\tilde{T}$ is added to account for values of the Weber number close to 1/3. The coefficients for the terms with spatial variation are different because the slow variable ξ is constant at points moving with the group velocity; adding $c_g\partial/\partial\xi$ to $\partial/\partial\tilde{t}$ leads to the same terms as in McGoldrick (1970). For large $|\tilde{T}|$, equations (111)-(112) are consistent with previous results. As $|\tilde{T}| \to \infty$, (112) reduces to

$$A_2 = \frac{A_1^2}{3i\tilde{T}}, \tag{113}$$

which, with (107), is found to agree with (85). Using (113) to remove A_2 in (111) gives

$$iA_{1\tilde{t}} = -\frac{1}{3\tilde{T}} |A_1|^2 A_1. \tag{114}$$

This equation can also be obtained from (104) by using (107), setting $\tau = a\tilde{t}$, and noting that the dissipation and the dispersion terms become small as $T \to 1/3$. Thus, the results for $T \neq 1/3$ and for T close to $1/3$ match asymptotically as $T \to 1/3$ and $|T - 1/3|/a \to \infty$.

A set of solutions of (111)-(112) for infinite wavetrains without ξ-dependence can be obtained as

$$A_1 = b_0 e^{-i\theta\tilde{t}} \tag{115}$$

$$A_2 = i\left(\frac{b_0}{b_0^c}\right)\theta e^{-2i\theta\tilde{t}}, \tag{116}$$

where

$$\theta = \frac{1}{8}\left(3\tilde{T} - (\mathrm{sgn}\tilde{T})\sqrt{9\tilde{T}^2 + 16\,|b_0|^2}\right), \tag{117}$$

and b_0 is a complex constant. The sign in (117) has been chosen so that $\theta \to 0$ when $|\tilde{T}| \to \infty$. Then, also $|A_2| \to 0$, and hence b_0 becomes identical to a_0 as $|\tilde{T}| \to \infty$. When $\tilde{T}$ is zero, the wavetrains obtained by McGoldrick (1970) are recovered from (115)-(117).

A nonuniformity related to the third-harmonic resonance is observed when $T = 1/4$. We can expect more nonuniformities for $T = 1/(n+1)$ $(n = 3, 4, \cdots)$, corresponding to a n^{th}-harmonic resonance. Uniform expansions near these resonance values of the Weber number can be obtained by modifying those introduced for $T = 1/3$ above. The amplitude equation (104) still can describe the evolution of the slowly varying amplitude of the first-order solutions, because higher-harmonic corrections need not be imposed on the first-order solutions (Joo et al., 1989).

Still another nonuniformity occurs for values of T close to unity, when the surface-tension force is large in comparison with the gravitational force. In this case, the long-wave solutions for the velocity potential and the surface elevation must be modified. Since the orders of magnitude change, it is now convenient to omit subscripts and to denote the largest "long-wave" terms by $\epsilon^{1/2}\phi^0$ and $\epsilon^{1/2}\eta^0$, where ϕ^0 and η^0 are not necessarily $O(1)$. By repeating the previous

derivations when $1-T \ll 1$, we find that the equations analogous to (98) and (103) become

$$-\frac{1+2T}{2}\eta^0_\xi + \phi^0_y = 2(1-T)\frac{\partial\,|A|^2}{\partial\xi} - i(Q_0 A A^c_\xi - Q^c_0 A^c A_\xi) \tag{118}$$

$$(1-T)\eta^0 = \frac{1+2T}{2}\epsilon^{1/4}\phi^0_\xi. \tag{119}$$

When $1-T = O(1)$, then $\phi^0 = O(1)$ but $\eta^0 = O(\epsilon^{1/4})$; η^0 and ϕ^0 can be replaced by $\epsilon^{1/4}\eta^0_3$ and ϕ^0_2, respectively, and (98) and (103) are recovered. When $\epsilon^{1/4} \ll 1-T \ll 1$, $\eta^0 = O\{\epsilon^{1/4}/(1-T)\}$ while ϕ^0 remains $O(1)$. In the distinguished limit corresponding to $1-T = O(\epsilon^{1/4})$, all terms in (118) and (119) are retained. Finally, for $1-T \ll \epsilon^{1/4}$, $\eta^0 = O(1)$ while $\phi^0 = O(\{(1-T)/\epsilon^{1/4}\})$. Thus, for pure capillary disturbances in the presence of a surfactant, there is a long-wave component with a surface elevation $\epsilon^{1/2}\eta^0(\xi,\tau)$, whereas the corresponding long-wave potential is of higher order; η^0 is determined by (118). For a clean surface, however, the nonuniformity at $T=1$ disappears because $Q_0 = 0$ and ϕ^0_2 is proportional to $1-T$.

5 Linear stability analysis

The effects of viscosity and surfactant on the stability of infinite wavetrains to sideband disturbances of the Benjamin-Feir type can be examined by considering the dissipative NLS equations (65) and (104). We can obtain the evolution of disturbances to the solutions (66) and (105) for small time, while the magnitude of the disturbances stays relatively small, by extending the linear analysis of Stuart & DiPrima (1978); this extension incorporates the unsteadiness of the basic state.

We first consider a perturbation to the wavetrain (66) for gravity waves and write

$$A = A_0(\tau)\,[1 + B(\xi,\tau)]\,. \tag{120}$$

Substituting (120) into (65) gives

$$iB_\tau - \frac{1}{8}B_{\xi\xi} = 2\,|a_0|^2\, e^{-4\lambda^2\tau}(B + B^c) \tag{121}$$

after the quadratic terms in B are neglected. For a pair of sideband modes, we seek a solution

of (121) in the form

$$B = B_1(\tau)e^{il\xi} + B_2(\tau)e^{-il\xi}, \tag{122}$$

where B_1 and B_2 are complex coefficients, and l is a real wavenumber.

Although the disturbance can grow for small values of the slow time variable τ, it will eventually be damped out due to viscous dissipation. A norm for one spatial period,

$$N(\tau) = \Big\| \, |A| - |A_0| \, \Big\| \equiv \sqrt{\frac{l}{2\pi} \int_{-\pi/l}^{\pi/l} (|A| - |A_0|)^2 \, d\xi}, \tag{123}$$

can be used as a measure of the growth or decay of the disturbance. While the magnitude of the disturbance B stays small, the norm N is equivalent to

$$N(\tau) = \frac{|A_0|}{\sqrt{2}} \left(|B_1|^2 + |B_2|^2 + B_1 B_2 + B_1^c B_2^c \right)^{1/2}, \tag{124}$$

which is seen by substituting (120) and (122) into (123).

We now substitute (122) into (121) and obtain a pair of linear homogeneous equations for B_1 and B_2:

$$B_1' - \frac{il^2}{8} B_1 + 2i \, |a_0|^2 \, e^{-4\lambda^2\tau} (B_1 + B_2^c) = 0 \tag{125}$$

$$B_2' - \frac{il^2}{8} B_2 + 2i \, |a_0|^2 \, e^{-4\lambda^2\tau} (B_1^c + B_2) = 0, \tag{126}$$

where a prime denotes differentiation with respect to τ. Equations (125)-(126) and the transformation

$$B_1 = e^{-2\lambda^2\tau} \bar{B}(\tau) \tag{127}$$

yield

$$\bar{B}'' - \theta \bar{B} = 0, \tag{128}$$

where

$$\theta = \frac{l^2}{64} (32 \, |a_0|^2 \, e^{-4\lambda^2\tau} - l^2) + \frac{i}{2} \lambda^2 l^2 + 4\lambda^4. \tag{129}$$

In the inviscid limit ($\lambda \to 0$), $|A_0|$ is constant, and (129) becomes

$$\theta = \frac{l^2}{64} (32 \, |a_0|^2 - l^2) \tag{130}$$

and $\bar{B} = B_1$. The stability of the flow is then determined by the sign of θ: $\theta > 0$ indicates instability, whereas $\theta < 0$ gives neutral stability, in agreement with the inviscid instability condition of Benjamin & Feir (1967):

$$0 < l^2 < 32\,|a_0|^2\,. \tag{131}$$

The details of the instability for inviscid flow were given by Stuart & DiPrima (1978).

When viscosity is present, the solution for $\bar{B}$ is obtained from (128). A change of variables

$$s = \frac{|a_0|\,l}{2\sqrt{2}\lambda^2} e^{-2\lambda^2\tau} \tag{132}$$

leads to the Bessel equation

$$s^2\frac{d^2\bar{B}}{ds^2} + s\frac{d\bar{B}}{ds} - (s^2 + \alpha^2)\bar{B} = 0, \tag{133}$$

where

$$\alpha = 1 + i\frac{l^2}{16\lambda^2}. \tag{134}$$

The solution for $\bar{B}$ is

$$\bar{B} = c_1 K_\alpha(s) + c_2 I_\alpha(s), \tag{135}$$

where K_α and I_α are modified Bessel functions of complex order α, and c_1 and c_2 are constants to be determined by initial conditions at $s = |a_0|\,l/(2\sqrt{2}\lambda^2)$. For large τ, and thus small s, the disturbances are expected to decay as a result of viscous damping. As $s \to 0$, the Bessel functions in (135) have the form

$$K_\alpha(s) \sim (\text{constant})s^{-\alpha}, \qquad I_\alpha(s) \sim (\text{constant})s^{\alpha}. \tag{136}$$

The solution for $\bar{B}$, therefore, is

$$\bar{B} \sim (\text{constant})e^{il^2\tau/8}e^{2\lambda^2\tau} \tag{137}$$

as $\tau \to \infty$. However, since $B_1 = e^{-2\lambda^2\tau}\bar{B}$ and $|A_0| = a_0 e^{-2\lambda^2\tau}$, the amplitude of the disturbance as $\tau \to \infty$ is

$$|A_0 B_1| = O(e^{-2\lambda^2\tau}) \tag{138}$$

and approaches zero as anticipated.

The result (138) obviously does not allow recovery of the condition (131) obtained for zero viscosity. If λ is small, both the order and the argument of the Bessel functions are large in magnitude. To achieve a single asymptotic representation that contains (131) and also predicts decay for large time, we take the limit as $\lambda \to 0$ and $\tau \to \infty$ with $\lambda^2\tau$ fixed. Then,

$$K_\alpha(s) = \sqrt{\frac{\pi}{2\alpha}}\left(1+\frac{s^2}{\alpha^2}\right)^{-1/4}\exp\left[-\alpha\sqrt{1+\frac{s^2}{\alpha^2}}-\alpha\ln\frac{s/\alpha}{1+\sqrt{1+s^2/\alpha^2}}\right] \tag{139}$$

$$I_\alpha(s) = \frac{1}{\sqrt{2\pi\alpha}}\left(1+\frac{s^2}{\alpha^2}\right)^{-1/4}\exp\left[\alpha\sqrt{1+\frac{s^2}{\alpha^2}}+\alpha\ln\frac{s/\alpha}{1+\sqrt{1+s^2/\alpha^2}}\right]. \tag{140}$$

The previous results are now recovered for large and small values of $\lambda^2\tau$. If $\lambda^2\tau \to \infty$, the largest term arises from K_α and is proportional to $s^{-\alpha}$, as in (136); thus, $\bar{B}$ is again found in the form (137). If $\lambda^2\tau \to 0$,

$$\frac{s}{\alpha} = \frac{|a_0|\,l}{2\sqrt{2}\lambda^2\alpha}\left(1-2\lambda^2\tau+\cdots\right), \tag{141}$$

and $\bar{B}$, after some manipulation, becomes

$$\bar{B} \sim (\text{constant})\exp\left(\frac{il^2}{8}\sqrt{1-\frac{32\,|a_0|^2}{l^2}}\cdot\tau\right) + (\text{constant})\exp\left(-\frac{il^2}{8}\sqrt{1-\frac{32\,|a_0|^2}{l^2}}\cdot\tau\right). \tag{142}$$

This is exactly the solution of (128) when $\lambda = 0$.

The linear stability analysis for capillary-gravity waves represented by (105) proceeds in the same way as for the gravity wave. The evolution equation for the disturbance, equivalent to (121), becomes

$$iB_\tau - \frac{1}{8}(4T^2-8T+1)B_{\xi\xi} = \frac{1}{4}\frac{9T^2-15T+8}{1-3T}\,|a_0|^2\exp\left(-\frac{1}{\sqrt{2}}\frac{\kappa^2\lambda^2}{\kappa^2-\sqrt{2}\kappa+1}\tau\right)(B+B^c). \tag{143}$$

The transformation and definition for θ corresponding to (127) and (130) are

$$B_1 = e^{-D\lambda^2\tau}\bar{B}(\tau) \tag{144}$$

$$\theta = T_1 l^2\left(2\,|a_0|^2\,T_2 e^{-2D\lambda^2\tau} - T_1 l^2\right) + i2DT_1\lambda^2 l^2 + D^2\lambda^4, \tag{145}$$

respectively, where

$$D = \frac{1}{2\sqrt{2}} \cdot \frac{\kappa^2}{\kappa^2 - \sqrt{2}\kappa + 1}. \tag{146}$$

and

$$T_1 = \frac{4T^2 - 8T + 1}{8} \quad \text{and} \quad T_2 = \frac{9T^2 - 15T + 8}{4(1 - 3T)}. \tag{147}$$

For inviscid flow, (145) reduces to

$$\theta = T_1 l^2 \left(2 \left|a_0\right|^2 T_2 - T_1 l^2\right). \tag{148}$$

When $T_1 T_2 < 0$, or

$$1 - \frac{\sqrt{3}}{2} \leq T < \frac{1}{3}, \tag{149}$$

θ is always negative, and the side-band resonance disappears regardless of the disturbance wavenumber. The corresponding stability analysis for waves in water of finite depth has been reported by Djordjevic & Redekopp (1977). The stability band (149) corresponds to the deep-water limit of their stable region, which lies between the minimum phase speed and the second-harmonic resonance. The other stable regions seem to disappear as the depth approaches infinity. Although only neutral stability is predicted for (149), computations of the large-time modulation for this region, in the following section, show strikingly different behavior from that in the other neutrally stable regions. When $0 < T < 1 - \sqrt{3}/2$, the lower instability boundary for l stays at zero, whereas the upper bound increases with T until it blows up at $T = 1 - \sqrt{3}/2$. When the Weber number exceeds the value for the second-harmonic resonance, the upper bound decreases with the Weber number. As $T \to 1$, the upper bound approaches $l = 1/\sqrt{3}$, which is smaller than the value $l = 2\sqrt{2}$ for gravity waves.

For viscous flow, the solution for $\bar{B}$ with (145) should be considered. The change of variables analogous to (132) is

$$s = \frac{\sqrt{2T_1 T_2}\,|a_0|\,l}{D\lambda^2} e^{-D\lambda^2 \tau}. \tag{150}$$

The resulting equation is again the Bessel equation (135), but with

$$\alpha = 1 + i\frac{T_1 l^2}{D\lambda^2}. \tag{151}$$

The subsequent results are then similar to those for the gravity wave except that no initial growth is possible when the Weber number satisfies (149), as anticipated. A large-time modulation for this range of Weber numbers is examined in the following computations.

6 Numerical solution of dissipative NLS equations

The linear analysis in the previous section is valid only while the magnitude of the disturbance remains small. In this section, we obtain numerical solutions of (65) and (104) with given initial conditions and examine the evolution of a disturbance of the type in (122) for finite time.

Numerical solutions of the NLS equation have been obtained by Yuen & Ferguson (1978) and Weideman & Herbst (1987) and many others, with an emphasis on modulational instability and recurrence of the Fermi-Pasta-Ulam type (Fermi et al., 1974). Yuen & Ferguson (1978) examined the relationship between Benjamin-Feir instability and recurrence and showed two types of recurrence, "simple" and "complex." They explained that for modulations with the sideband perturbation wavenumber l in the range $8|a_0|^2 \leq l^2 < 32|a_0|^2$ the recurrence is simple because all higher harmonics of the prescribed modulation are stable. For modulations with $0 < l^2 < 8|a_0|^2$, the recurrence is complex (quasi-periodic) because at least one higher harmonic of the prescribed mode lies in the unstable region. Weideman & Herbst (1987) obtained similar solutions using finite-difference, spectral, and pseudospectral methods, and they compared the effectiveness of these methods. We use a pseudospectral method to solve the dissipative NLS equations for capillary-gravity waves. This method is appropriate for our purpose, once an aliasing error is suppressed by introducing a sufficient number of degrees of freedom (number of collocation points).

The initial condition (120), with B replaced by (122), is specialized to the simple case

$$A = a_0(1 + b\cos l\xi), \tag{152}$$

where the substitution

$$B_1(0) = B_2(0) = \frac{1}{2}b \tag{153}$$

has been made. Modulational behavior for different initial sideband amplitudes, B_1 and B_2, will be discussed later in this section.

A periodic boundary condition

$$A(\xi,\tau) = A(\xi + \frac{2\pi}{l},\tau), \tag{154}$$

is imposed using a Fourier-collocation method with the computational domain $-\pi/l \leq \xi \leq \pi/l$. The slowly varying amplitude is then expressed as

$$A = \sum_{n=-N}^{N} \tilde{A}_n(\tau) e^{in\xi\pi/l}, \tag{155}$$

where we choose N as a positive integer power of 2 and a fast Fourier transformation is used to compute the Fourier coefficients $\tilde{A}_n$. As in the analyses, the amplitude of a_0 is $\frac{1}{2}$, and b is small. In particular, we set $a_0 = \tilde{A}_0(0) = 0.5$ and $b = 2\tilde{A}_1(0) = 2\tilde{A}_{-1}(0) = 0.1$ for most of the computations, unless otherwise specified. A fourth-order Hamming modified predictor-corrector method is used for time marching. The fourth-order Runge-Kutta method is used for automatic adjustment of the initial time increment and for computation of starting values. For most computations, the maximum time step is 0.01, and the number of collocation points is 32 for one initial period in ξ.

Fig. 1 illustrates the evolution of the Stokes wave (67) for zero viscosity when subject to the modulation described by (152). Evolution of the envelope amplitude $|A(\xi,\tau)|$ is shown in Fig. 1a, c, and e, whereas the magnitude of each Fourier coefficient $|\tilde{A}_n(\tau)|$ $(n = 0, 1, 2, \cdots)$ is plotted in Fig. 1b, d, and f. Since $|\tilde{A}_n|$ is symmetric about $n = 0$ due to (152), the evolution for negative n is deleted for clarity. The perturbation wavenumber $l = 1$ corresponds to complex recurrence (Fig. 1a, b); $l = 2$ corresponds to the maximum initial growth rate and simple recurrence (Fig. 1c,d). These figures agree with the results of Yuen & Ferguson (1978) and Weideman & Herbst (1987), who provide detailed explanations. For the simple recurrence, the fundamental ($n = 0$) and sideband ($n = \pm 1$) modes are periodic, as can be also seen in Fig. 8. The higher modes (not shown in Fig. 8), excited due to nonlinear interaction, are not exactly periodic, but they are not dominant at any stage, making the modulation almost periodic in time.

When l lies outside of the instability range (131), a very nearly periodic oscillation is observed (Fig. 1e), which is in good agreement with the neutral stability predicted by the linear analysis. The corresponding Fourier-space solution (Fig. 1f) shows that none of the higher harmonics is excited and that the sidebands never become dominant.

In Fig. 2, the same cases as in Fig. 1 are described using the norm N defined in (123). The behavior for small τ is in precise agreement with the linear analysis. The growth rate is a maximum when $l = 2$ and decreases as l increases, resulting in larger recurrence periods, until it becomes zero for $l = 2\sqrt{2}$. When l becomes larger than $2\sqrt{2}$, an oscillation due to neutral stability is observed, as predicted by the linear analysis. When l decreases from 2, the initial growth rate again decreases, but complex recurrence is observed for $l < \sqrt{2}$.

Fig. 3 shows the evolution of the slowly varying envelope A for gravity waves with small viscosity. The initial condition and the perturbation wavenumber l are identical to those for the cases in Fig. 1. Here, the dissipative NLS equation (65) is solved with $\lambda = 0.125$. In Fig. 3a and 3b, the values of l lie in the instability range, and the initial behavior shows a modulational instability despite viscous dissipation, which is in agreement with the analysis in the previous section for small λ. Compared to the corresponding cases in Fig. 1, the spikes are attenuated at larger times for both the complex and the simple recurrence. In Fig. 3c, the value $l = 4$ lies outside the instability range.

The norm for viscous gravity waves is plotted in Fig. 4. In Fig. 4a, $\lambda = 0.125$ as in Fig. 3, and the dependence of the modulation on the perturbation wavenumber is examined. The amplitudes of the recurrence are attenuated, as is also seen in Fig. 3, and the spikes are smoother. The value $l = 0.05$ lies within the instability range in the inviscid limit ($\lambda = 0$), but shows decay in Fig. 4a. The effect of λ is illustrated in Fig. 4b with $l = 2$ fixed. As λ becomes larger, the amplitude and period of recurrence decrease; when $\lambda = 0.5$, we observe monotonic decay. Fig. 4c shows the effect of the disturbance amplitude b when $l = 2$. For small time the growth rate does not demonstrate amplitude dependence, whereas for larger time the recurrence period increases as b decreases. Other calculations for neutral stability (e.g., $l = 4$) show that the modulational

behavior is hardly affected by changes in b and is almost exclusively dependent on l, as expected from the linear analysis.

For capillary-gravity waves with surfactants, the dissipative NLS equation is given by (104). The coefficient for the dissipation term is independent of the surface tension T, and the coefficients for the dispersion and nonlinear terms depend only on T. The term that corresponds to the frequency change in the coefficient for the dissipation term can be absorbed in the carrier wave and does not contribute to the magnitude of the envelope wave. The qualitative behavior of the modulation is then expected to be identical to that for the gravity waves when T is outside of the range (149), for the so-called self-focussing type of NLS equation. When T is in the range (149), equation (104) is of the defocussing type. In this case, the long-time modulation exhibits quite different features from the simple oscillation with constant amplitude and frequency found for neutral stability of the self-focussing type. A discussion of self-focussing and defocussing NLS equations was given by Peregrine (1983).

Fig. 5 shows the evolution of inviscid capillary-gravity waves ($\kappa = \lambda = 0$). The perturbation wavenumber is chosen as $l = 2$, and four different values of surface tension are considered. For pure gravity waves ($T = 0$), the maximum growth rate and simple recurrence are observed as in Fig. 3. For pure capillary waves ($T = 1$), $l = 2$ lies outside of the instability region, as can be deduced from (148); thus, an oscillation is observed with constant amplitude and frequency. For $T = 0.1$, $l = 2$ is closer to the lower bound of the instability region $l = 0$, and so complex recurrence occurs. The value $T = 0.3$ lies between $1 - \sqrt{3}/2$ and $1/3$, and the modulation shows initial neutral stability, as predicted by the analysis. However, for large time an additional periodic behavior is observed. The large-scale period increases as l decreases, as can be seen in Fig. 6a, where $l = 1$ while the other parameters remain unchanged ($T = 0.3$ and $\kappa = \lambda = 0$). The corresponding profile for amplitude evolution is given in Fig. 6b. Initially, the behavior is similar to that for neutral stability, but the amplitude then gradually decreases and the frequency starts to change until the initial envelope disintegrates at about $\tau = 30$; still later, the original form of the envelope is almost completely recovered, near $\tau = 60$. Therefore, this phenomenon can

be referred to as recurrence, of a small-amplitude type different from the recurrence related to Benjamin-Feir instability.

In Fig. 7, we examine the effect of dissipation due to viscosity and a surfactant; $\lambda = 0.125$, $\kappa = \sqrt{2}$, and $l = 1/\sqrt{6}$. The perturbation wavenumber corresponds to the maximum growth rate $\sqrt{\theta}$ for inviscid pure capillary waves. The norm for the case $T = 1$ grows to a maximum at twice its initial value near $\tau = 50$ (Fig. 7a). When $T = 0.1$, the instability with complex recurrence is observed despite viscous dissipation, whereas for T slightly smaller than $1 - \sqrt{3}/2$ ($T = 0.1339$), the complex recurrence is suppressed by dissipation, and monotonic decay is observed. For $T = 0.3$, a disintegration of the wave envelope is obvious even with viscous damping, as can be seen clearly in the corresponding evolution profile in Fig. 7b. From Fig. 7, we can also deduce that the period of the disintegration-recovery has increased from that in Fig. 6 because a smaller l has been considered.

In all the calculations above, the initial condition used is (152), which corresponds to a symmetric amplitude modulation. We now consider more general modulations by using (121) instead, with $B_1(0)$ and $B_2(0)$ not necessarily equal and real as in (152). For simplicity, the results for inviscid gravity waves are presented in Fig. 8. Only the dominant fundamental and the sideband modes are plotted. In all the cases considered, the wavenumber perturbation is $l = 2$, so that all exhibit an initial Benjamin-Feir instability followed by simple recurrence. In Fig. 8a, the given initial condition is identical to that in Fig. 1a and b, and so the results are identical. In Fig. 8b, it is obvious that the phase difference changes the modulational behavior significantly, including the recurrence period. Fig. 8c shows the effect of different initial sideband amplitudes, here showing an increase in the recurrence period with a decrease in amplitude. In Fig. 8c, only one of the sideband modes is present initially, but subsequent evolution shows that the other mode is automatically excited to produce the Benjamin-Feir instability. The initially different sideband amplitudes in Fig. 8c become nearly identical, as predicted by Stiassnie & Kroszynski (1982), but they recover their difference periodically in the subsequent recurrence.

7 Concluding remarks

The methods of multiple scales and matched asymptotic expansions have been used in a formal derivation of evolution equations for weakly nonlinear viscous water waves. The result is the nonlinear Schrödinger equation with an additional linear dissipation term. For both gravity waves and capillary-gravity waves with an insoluble surfactant, the largest terms in the damping coefficients are identical to classical linear results. For capillary-gravity waves, nonuniformities are observed despite dissipation due to the surfactant. Near the second-harmonic resonance, a modified set of evolution equations is obtained, which are matched asymptotically with the nonresonant results. For pure capillary waves, a rescaling of the long-scale free-surface elevation is required in the presence of surfactants.

The derived evolution equations are solved analytically and computationally to examine the modulation of infinite wavetrains with sideband disturbances of the Benjamin-Feir type. The linear analysis shows that in the presence of dissipation the modulation, described by modified Bessel functions of complex order, has the same initial behavior as the inviscid case but eventually decays to zero. In the inviscid limit, the instability condition obtained originally by Benjamin & Feir (1967) is recovered for gravity waves, whereas a stable range of Weber number is found for capillary-gravity waves, which agrees with that obtained by Djordjevic & Redekopp (1977). In this range, spectral computations show a new type of recurrence not directly related to the Benjamin-Feir instability.

This work was supported by the Program in Ship Hydrodynamics at The University of Michigan funded by the University Research Initiative of the Office of Naval Research Contract N000184-86-K-0684, ONR Ocean Engineering Contract N00014-87-0509. The authors acknowledge Professor J. Boyd for his valuable references and help in computations.

REFERENCES

Addison, J. V. and Schechter, R. S. 1979 An experimental study of the rheological behavior of surface films. *AIChE Journal*, **25**, 32-41.

Benjamin, T. B. and Feir, J. E. 1967 The disintegration of wave trains on deep water. *J. Fluid. Mech.*, **27**, 417-430.

Craik, A. D. D. 1982 The drift velocity of water waves. *J. Fluid. Mech.*, **116**, 187-205.

Davey, A. and Stewartson, K. 1974 On three-dimensional packets of surface waves. *Proc. R. Soc. London A*, **338**, 101-110.

Djordjevic, V. D. and Redekopp, L. G. 1977 On two-dimensional packets of capillary-gravity waves. *J. Fluid Mech.*, **79**, 703-714.

Fermi, E., Pasta, J., and Ulam, S. 1965 **Collected papers of Enrico Fermi**. Edited by Segre, E. University of Chicago, Chicago, **2**, 978.

Garrett, W. D. 1986 ONRL Report C-11-86, 1-17.

Goodrich, F. C. 1960 The mathematical theory of capillarity I-III. *Proc. Roy. Soc. London A*, **260**, 481-509.

Goodrich, F. C. 1962 On the damping of water waves by monomolecular films. *J. Phys. Chem.*, **66**, 1858-1863.

Hasimoto, H. and Ono, H. 1972 Non-linear modulation of gravity waves. *J. Phys. Soc. Japan*, **33**, 805.

Joo, S.-W., J. Huh, W.W. Schultz (1989) Capillary-gravity water wave resonance. in preparation.

Lamb H. 1932 **Hydrodynamics**, 6^{th} ed. Cambridge University Press.

Levich, V. G. 1941 *Zh. Eksperim. Theor. Fiz.*, **11**, 340.

Levich, V. G. 1962 **Physicochemical Hydrodynamics**, Prentice-Hall.

Liu, A.-K. and Davis, S. H. 1977 Viscous attenuation of mean drift in water waves. *J. Fluid. Mech.*, **81**, 63-84.

Lucassen-Reynders, E. H., and Lucassen, J. 1969 Properties of capillary waves. *Adv. Colloid Interface Sci.*, **2**, 347-395.

Lucassen, J. 1982 Effect of surface-active material on the damping of gravity waves: a reappraisal. *J. Colloid Interface Sci.*, **85**, 52-58.

Longuet-Higgins, M. S. 1953 Mass transport in water waves. *Phil. Trans. R. Soc. London A*, **245**, 535-581.

McGoldrick, L. F. 1970 On Wilton's ripples: a special case of resonant interactions. *J. Fluid Mech.*, **42**, 193-200.

Mei, C.C. 1983 **The Applied Dynamics of Ocean Surface Waves**, Wiley.

Peregrine, D. H. 1983 Water waves, nonlinear Schrödinger equations and their solutions. *J. Austral. Math. Soc. B*, **25**, 16-43.

Pereira, N. R. and Stenflo, L. 1977 Nonlinear Schrödinger equation including growth and damping. *Phys. Fluids*, **20**, 1733-1734.

Phillips, O. M. 1966 **Dynamics of the upper ocean.** Cambridge Univ. Press.

Pliny, 77 A.D. **Naturalis Historia.** Book ii, Chapter 107, section 234.

Reynolds, O. 1880 On the effect of oil on destroying waves on the surface of water. *Br. Assoc. Rept.; Papers*, **1**, 409.

Stiassnie, M and Kroszynski, U. I. 1982 Long-time evolution of an unstable water-wave train. *J. Fluid Mech.*, **116**, 207-225.

Stuart, J. T. and DiPrima, R. C. 1978 The Eckhaus and Benjamin-Feir resonance mechanisms. *Proc. R. Soc. London A*, **362**, 27-41.

Ünlüata, U. and Mei, C. C. 1970 Mass transport in water waves. *J. Geophys. Res.*, **75**, 7611-7618.

Weideman, J. A. C. and Herbst, B. M. 1987 Recurrence in semidiscrete approximations of the nonlinear Schrödinger equation. *SIAM J. Sci. Stat. Comput.*, **8**, 988-1004.

Whitham, G. B. 1967 Nonlinear dispersion of water waves. *J. Fluid Mech.*, **27**, 399-412.

Yuen, H. C. and Ferguson, W. E. 1978 Relationship between Benjamin-Feir instability and recurrence in the nonlinear Schrödinger equation. *Phys. Fluids*, **21**, 1275-1278.

Zakharov, V. E. 1968 Stability of periodic waves of finite-amplitude on the surface of deep fluid. *J. Appl. Mech. Tech. Phys.*, **9**, 190-194.

LIST OF FIGURES

($\lambda = 0.125$) and surfactant ($\kappa = \sqrt{2}$) when the perturbation wavenumber $l = 1/\sqrt{6}$ and the Weber number is chosen as: a) $T = 0.1$ (——), $T = 0.1339$ (- - - -), $T = 0.3$ (— · —), and $T = 1$ (· · · · · ·) b) $T = 0.3$.

Figure 8. Evolution of dominant Fourier modes ($n = 0$ and ± 1) for inviscid gravity waves when $l = 2$. The initial sideband amplitudes are represented by: a) $B_1 = 0.05$ and $B_2 = 0.05$, b) $B_1 = 0.05$ and $B_2 = 0.05\,i$, c) $B_1 = 0.05$ and $B_2 = 0$.

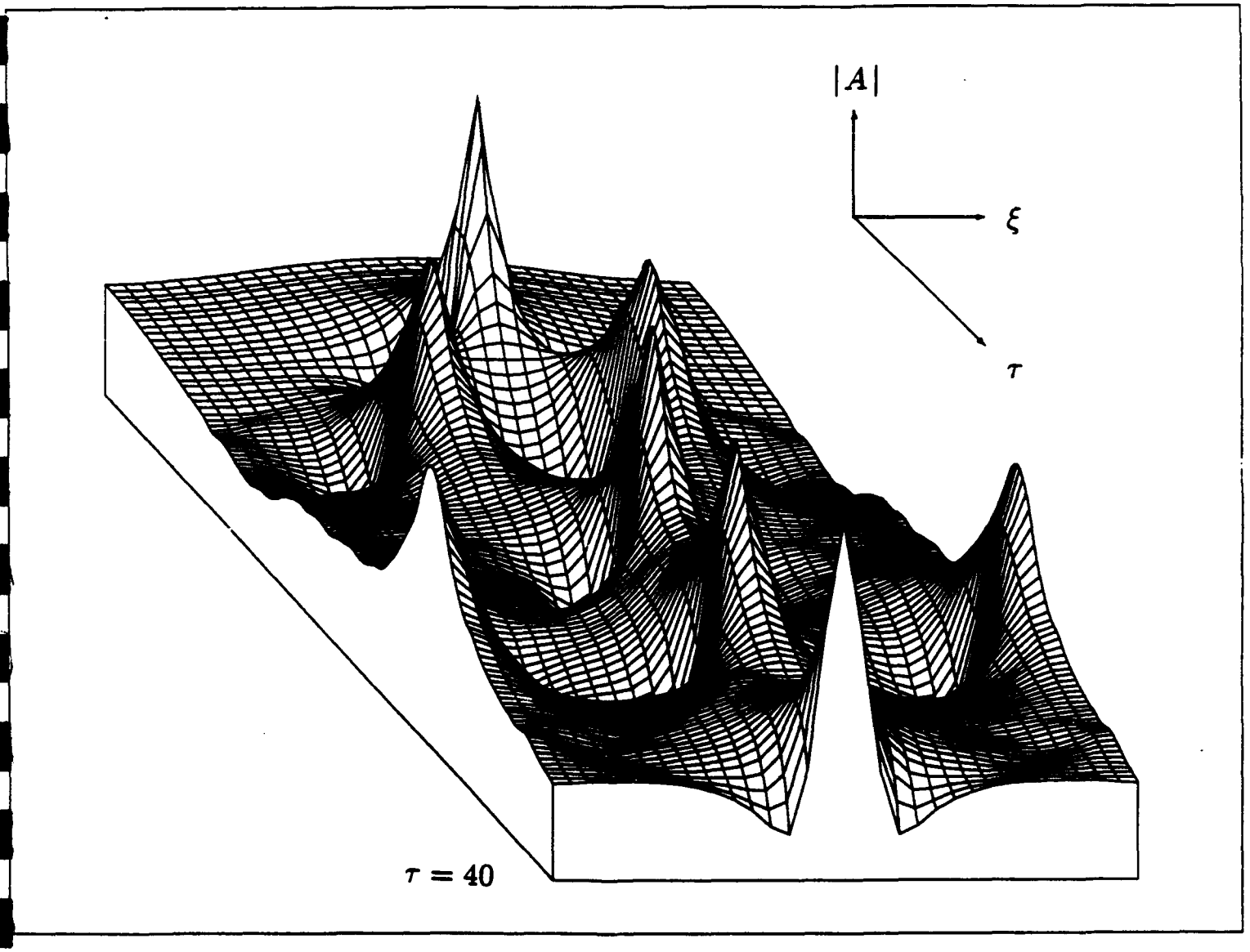

Fig 1a

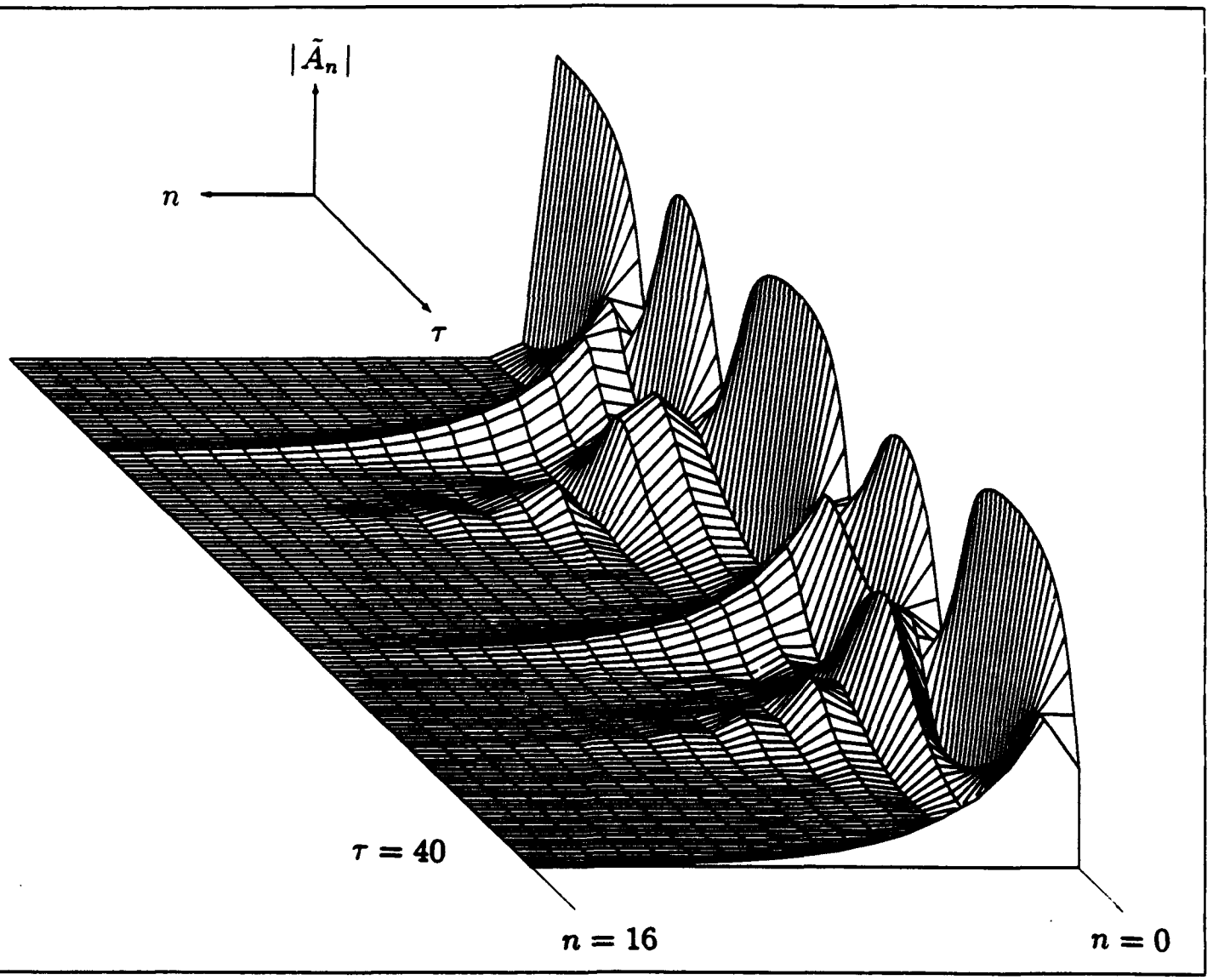

Fig 16

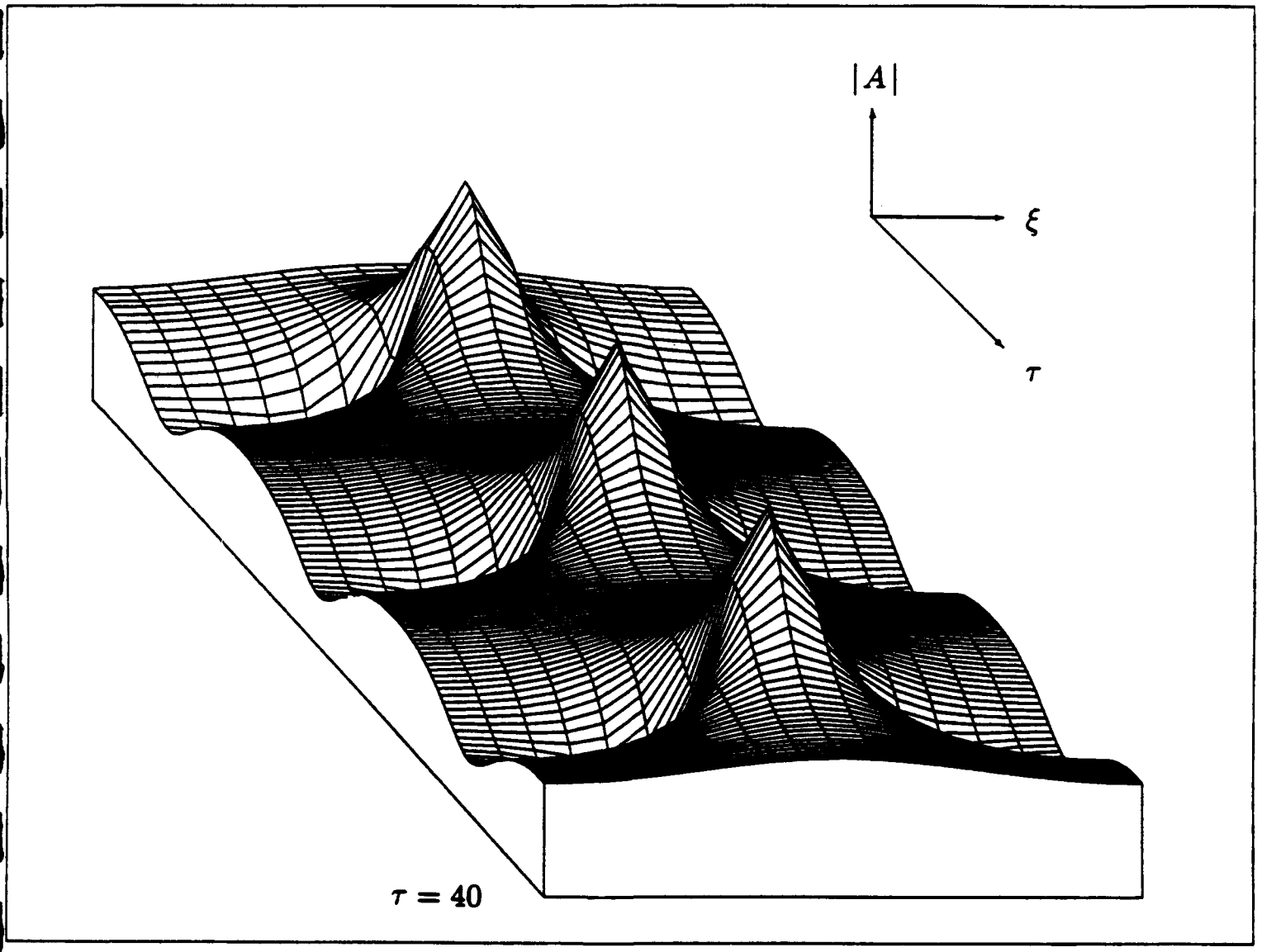

Fig 1C

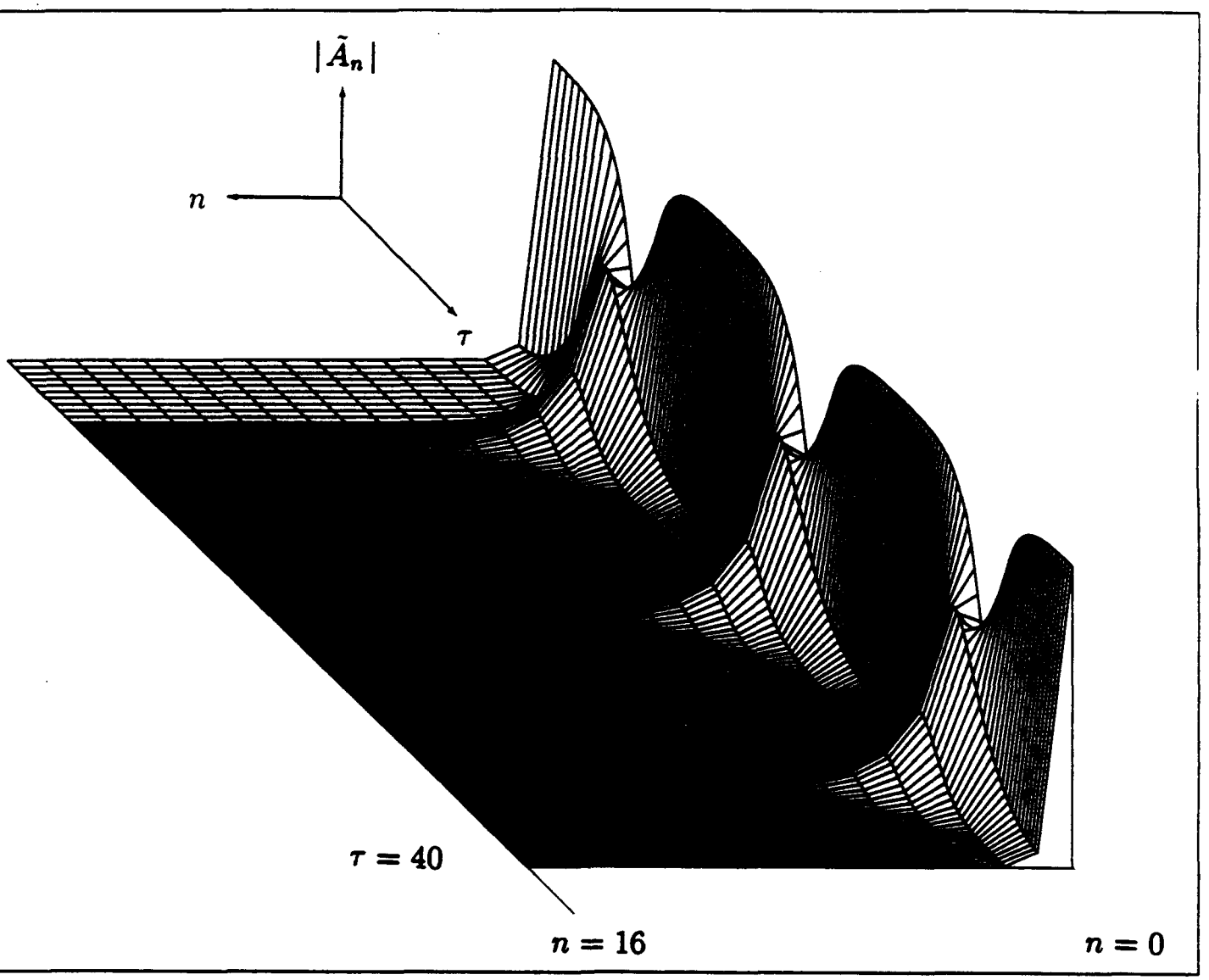

Fig 1d

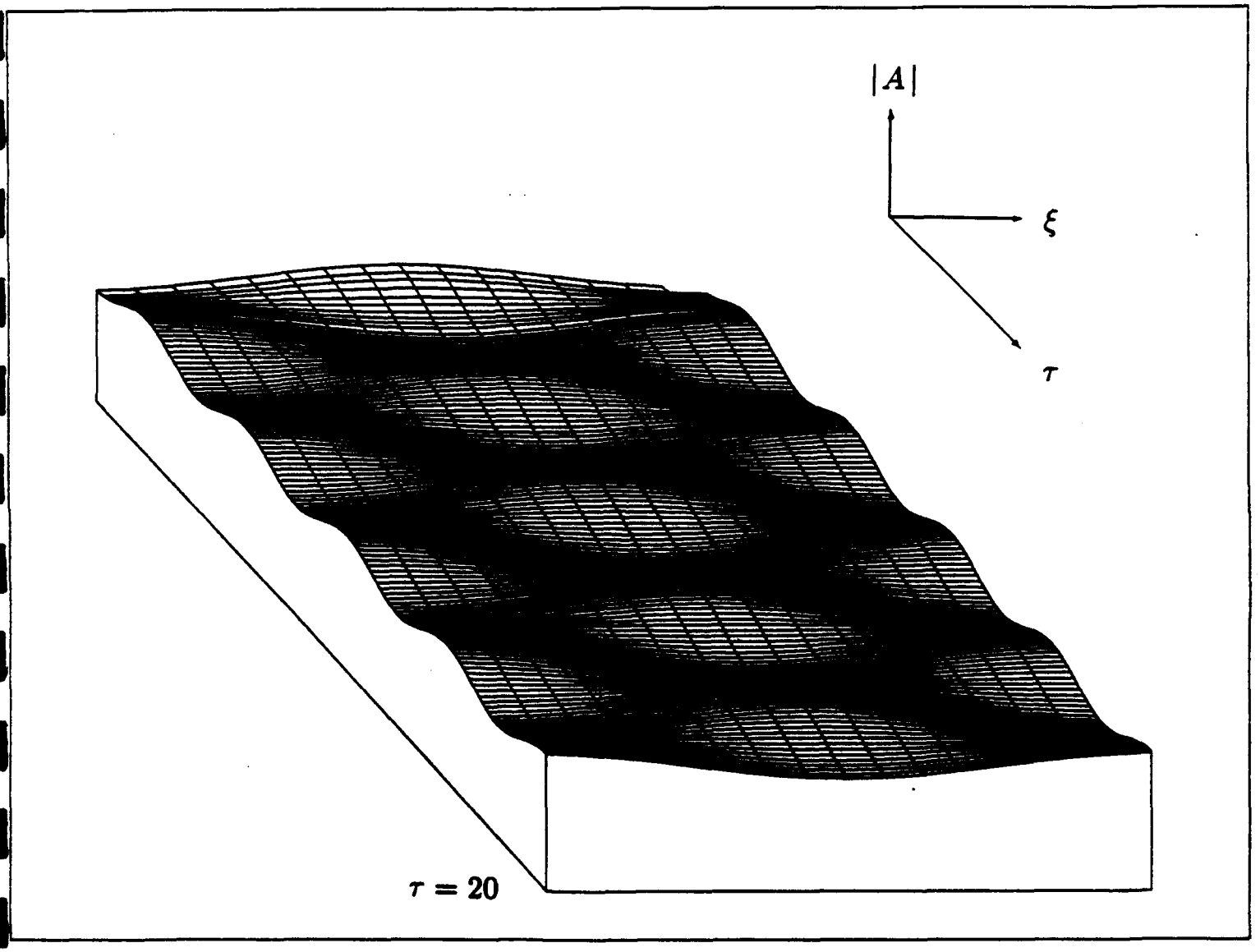

Fig 1e

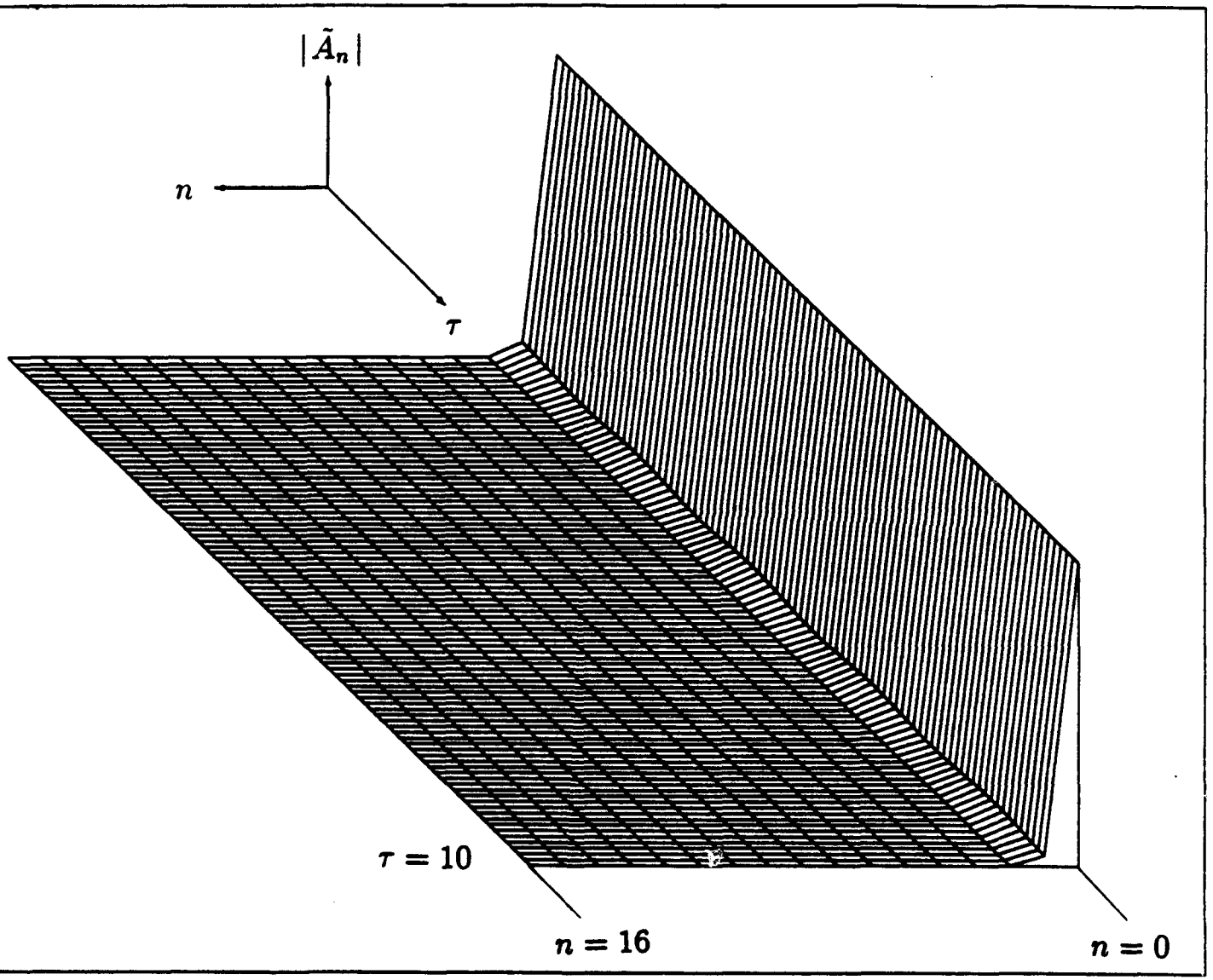

Fig 1f

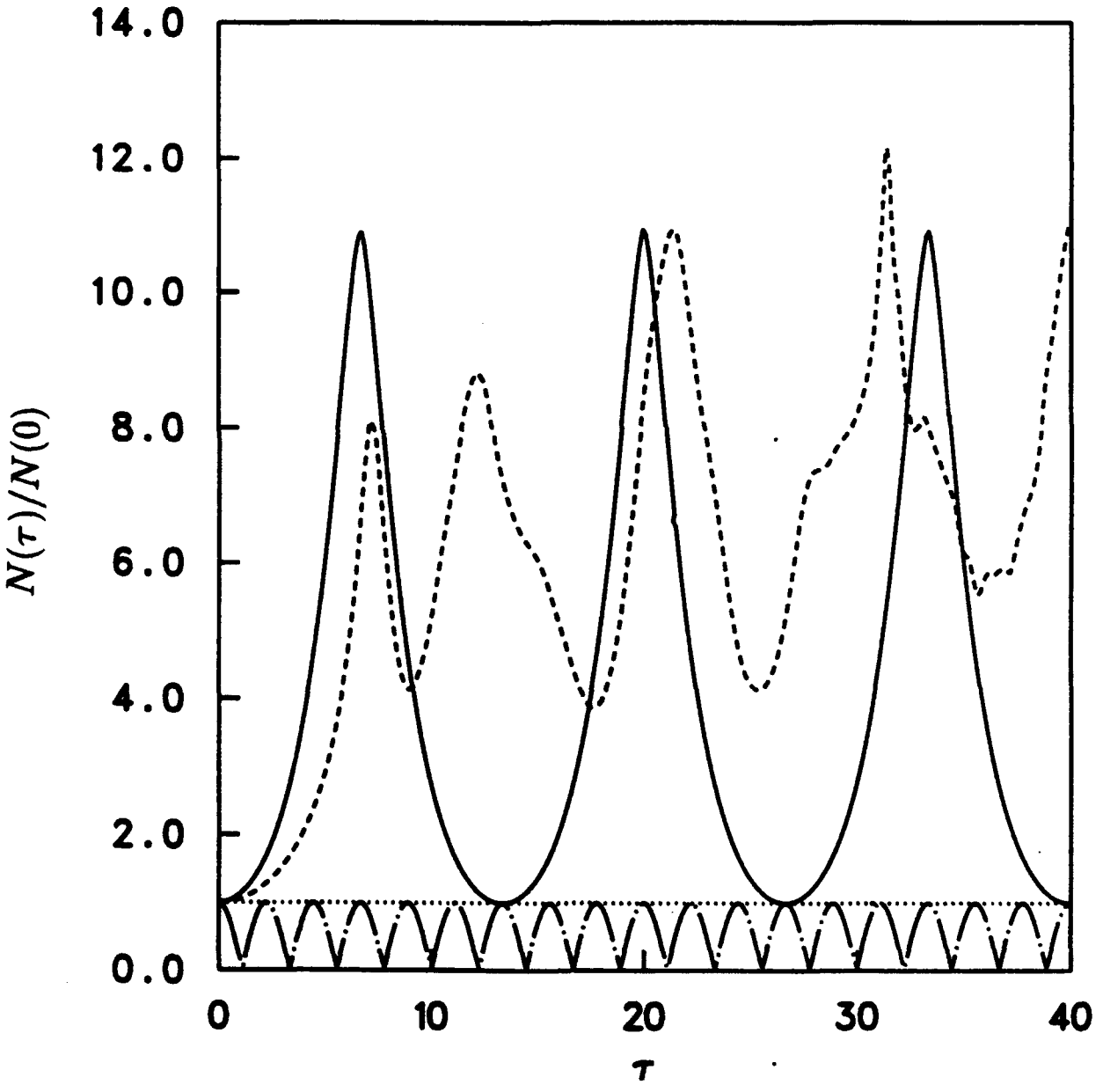

Fig. 2

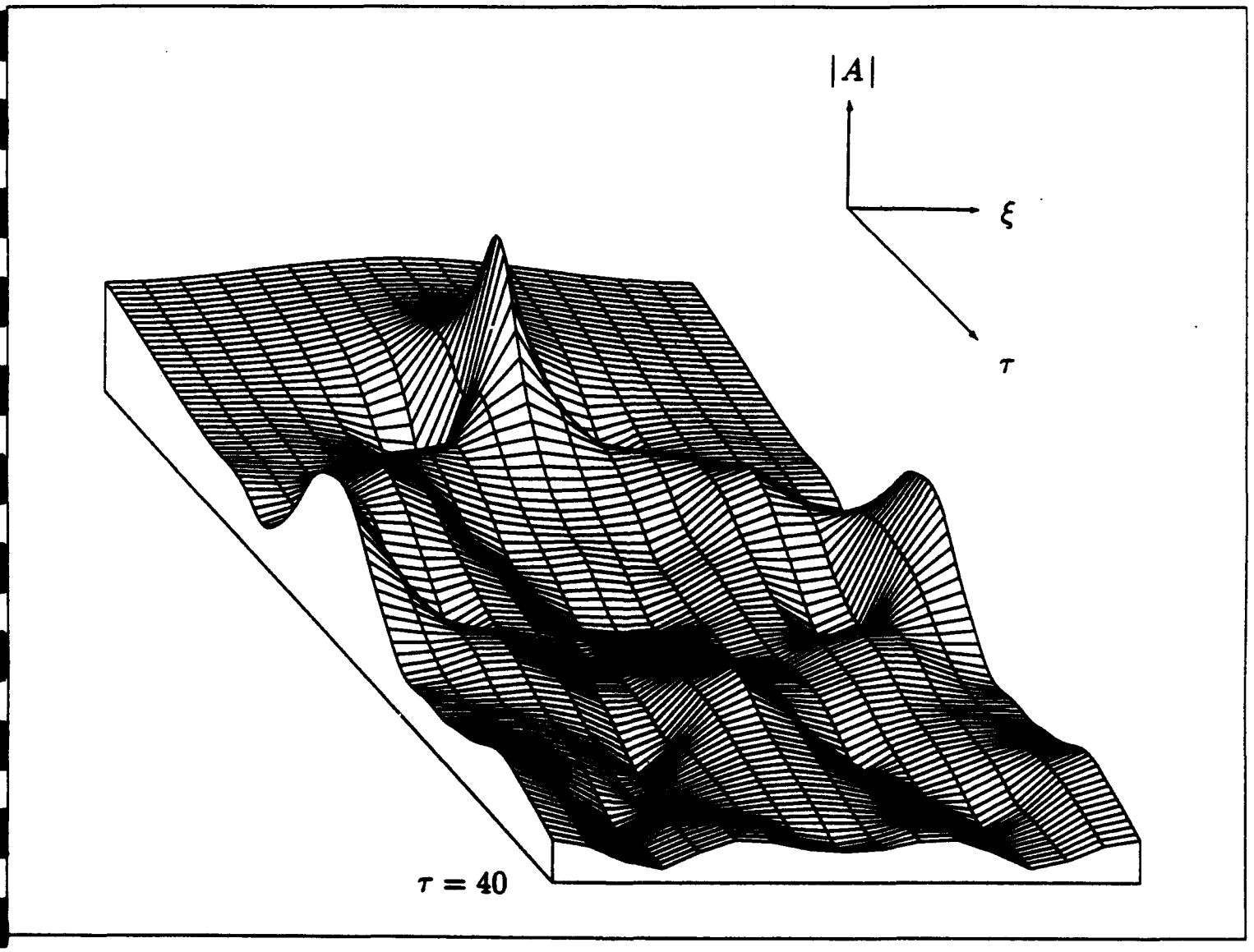

Fig 39

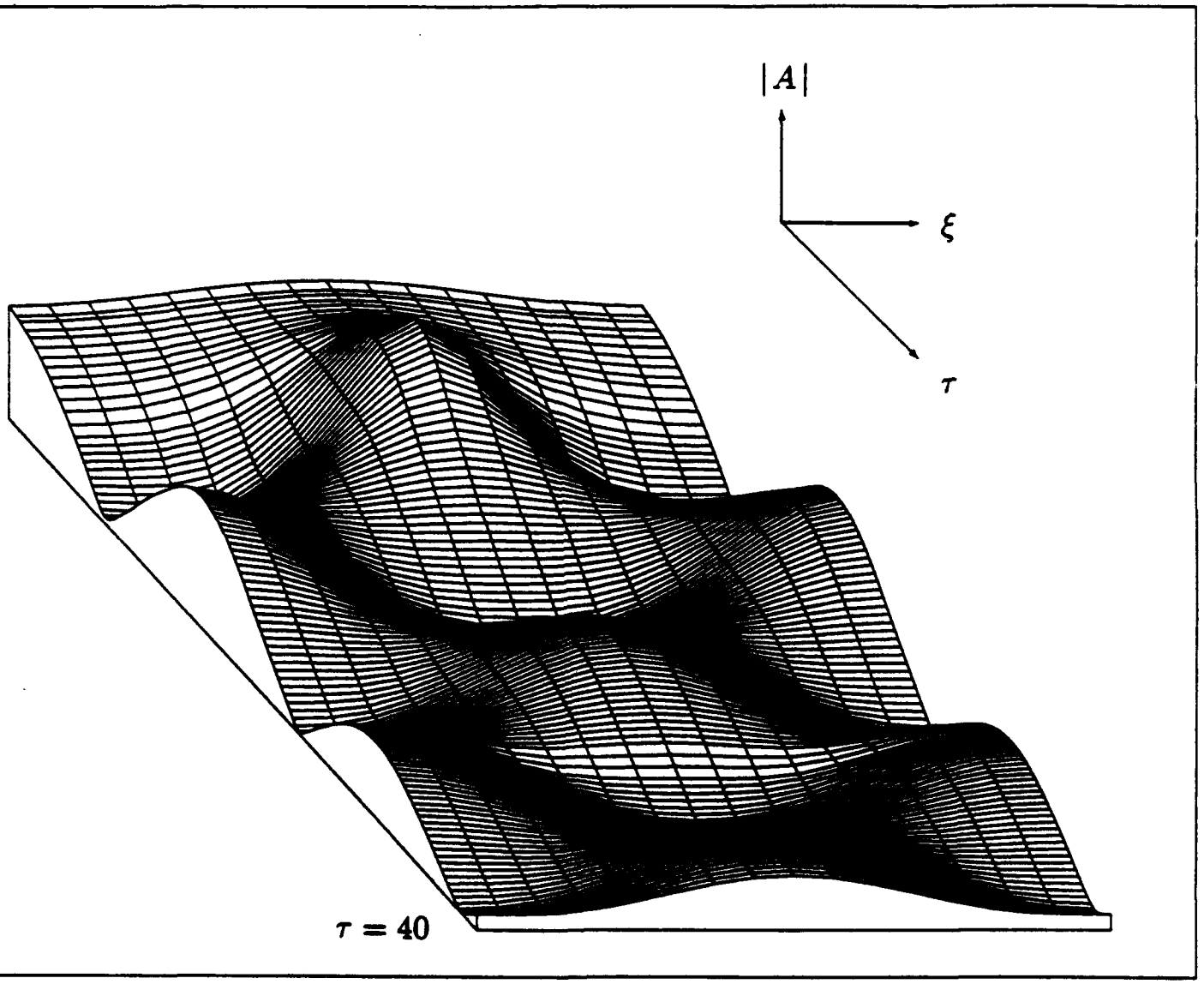

Fig 3b

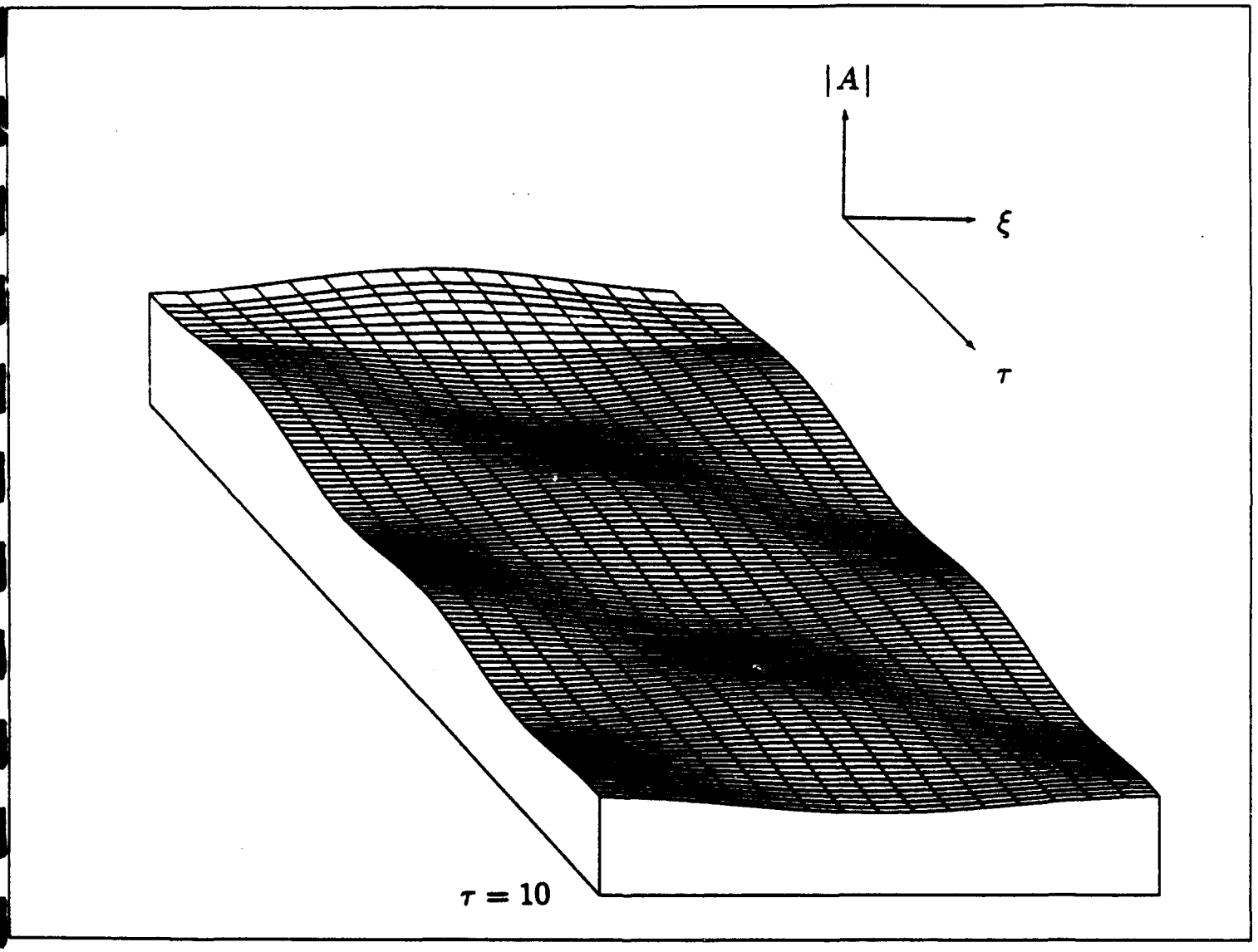

Fig 3C

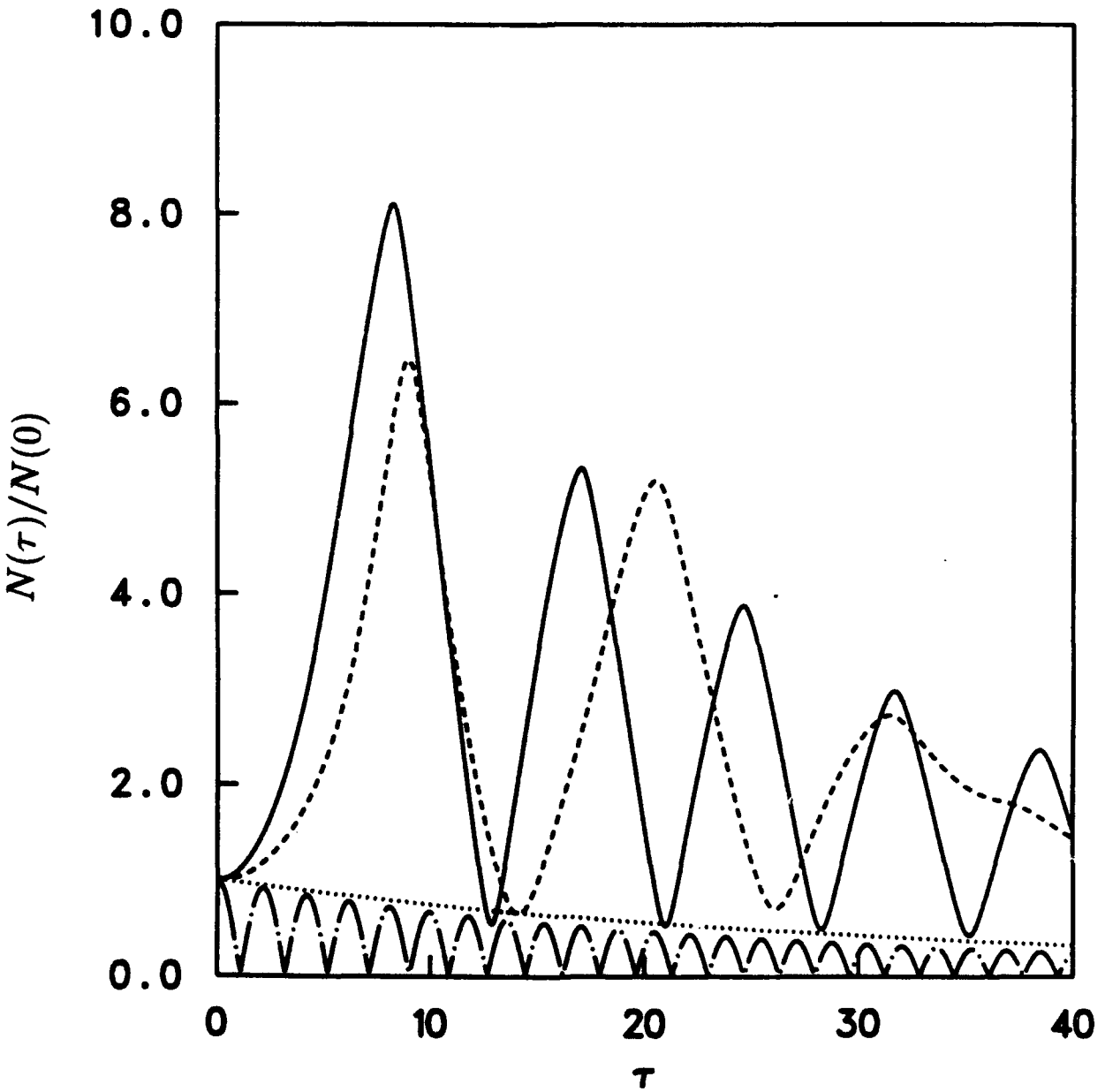

Fig. 4a

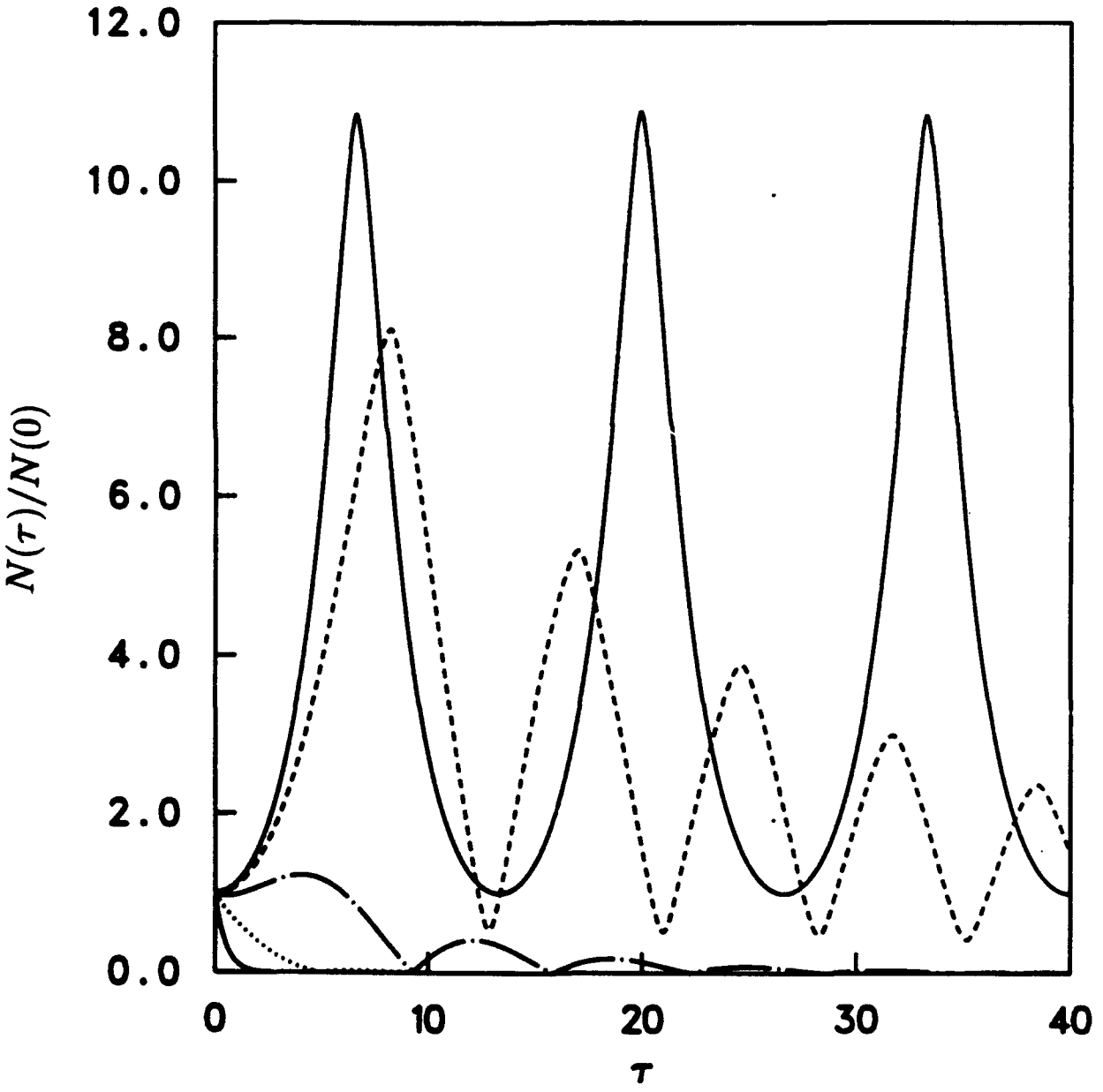

Fig. 4b

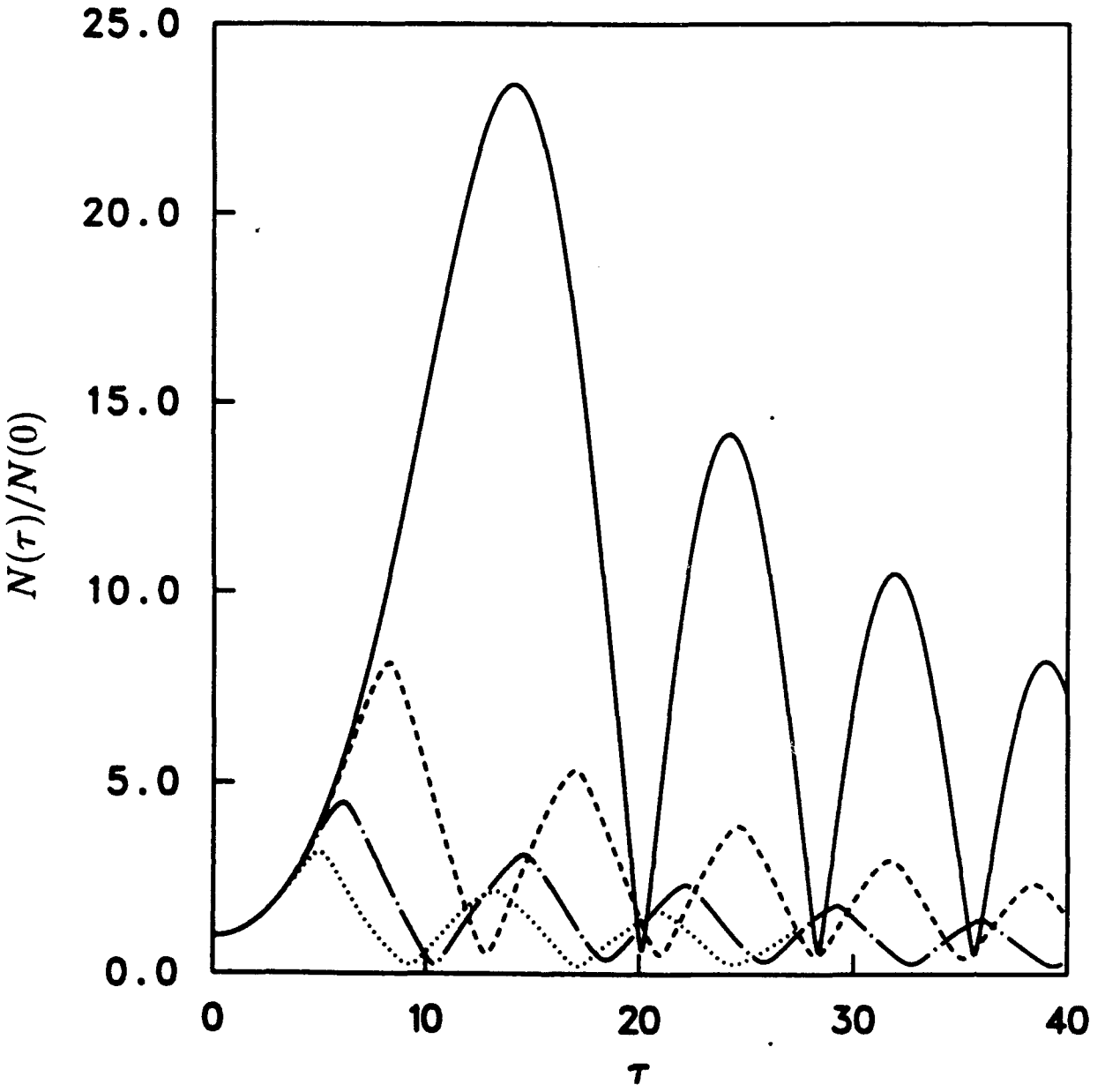

Fig. 4C

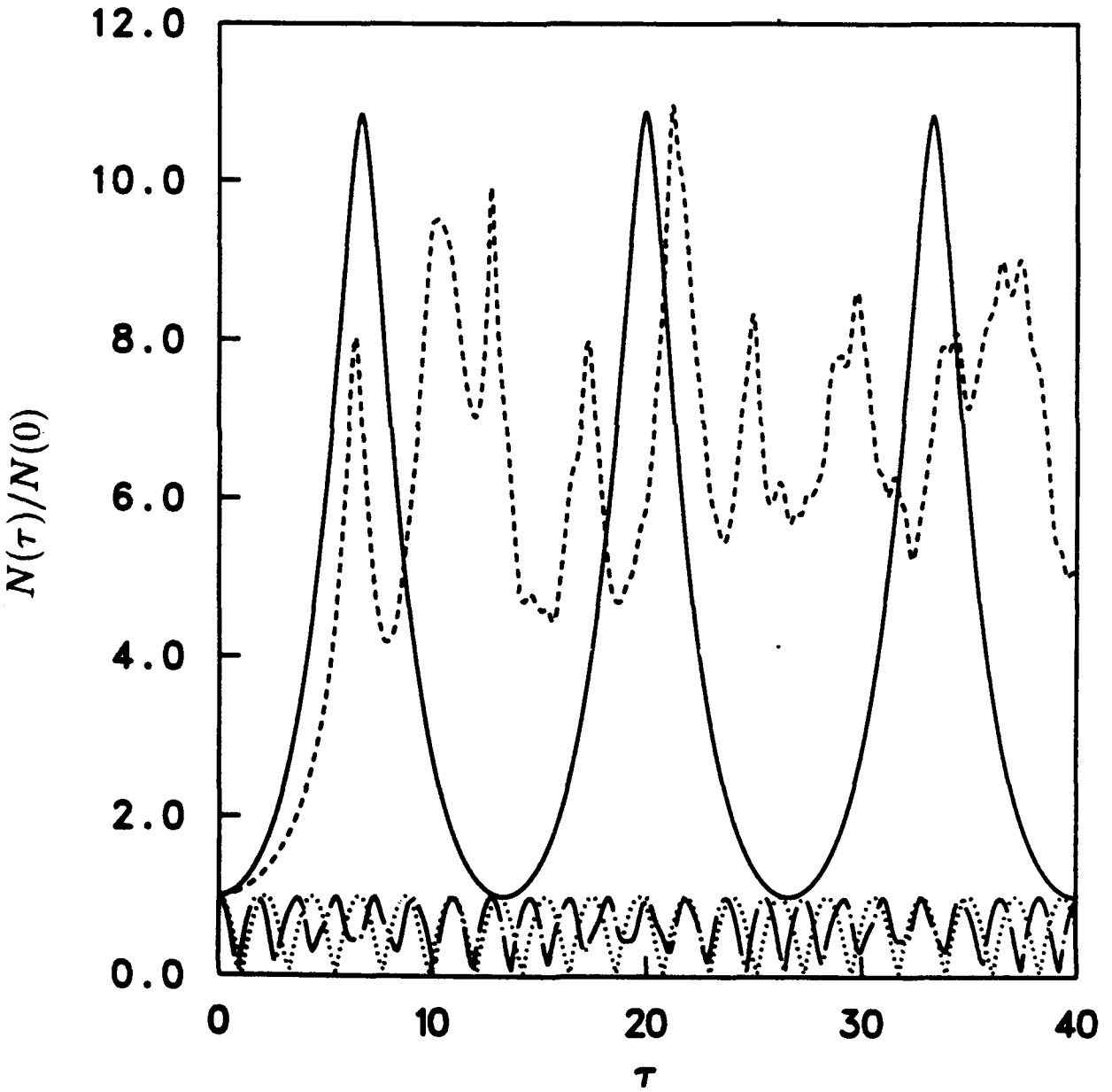

Fig. 5

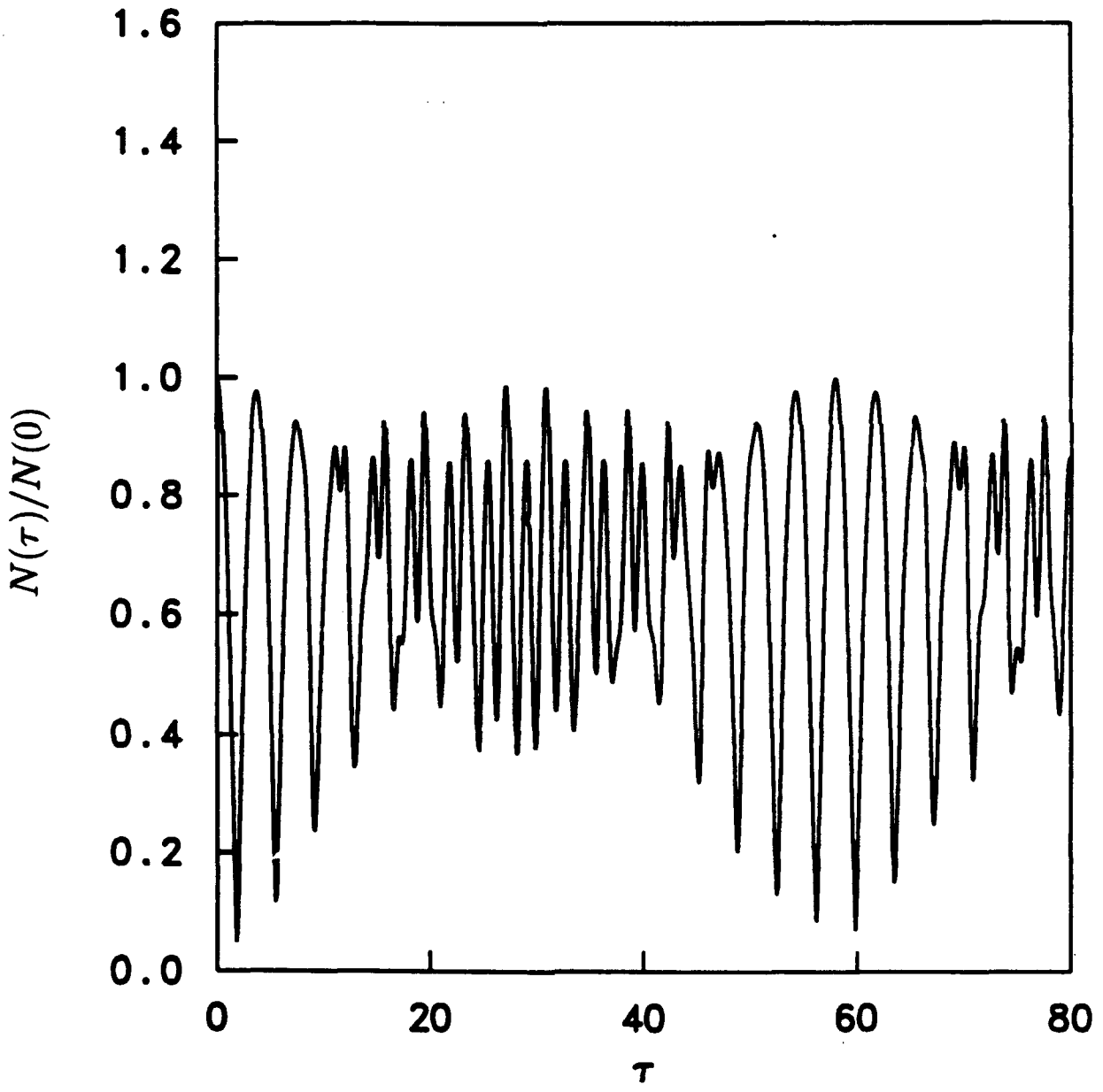

Fig. 6a

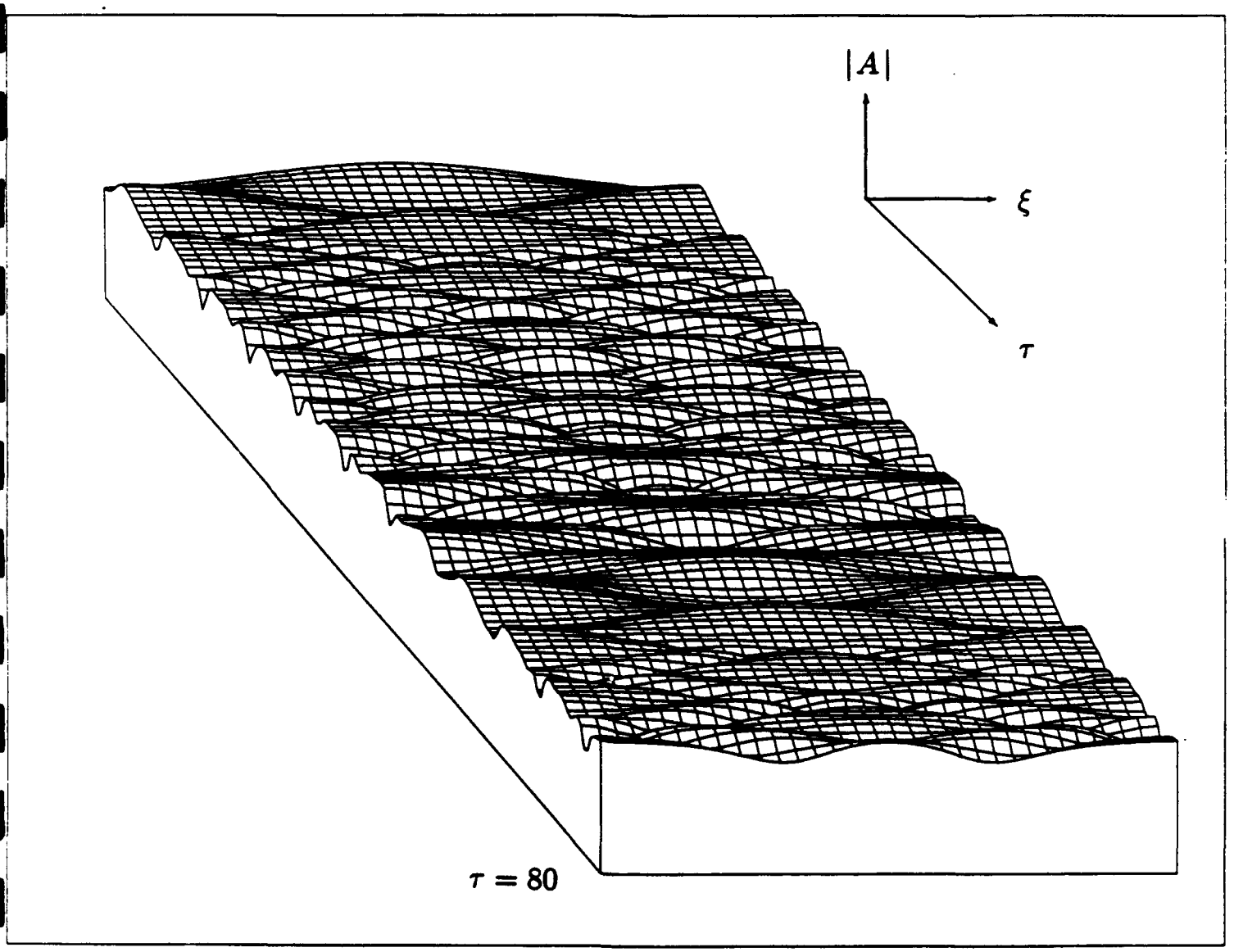

Fig 6b

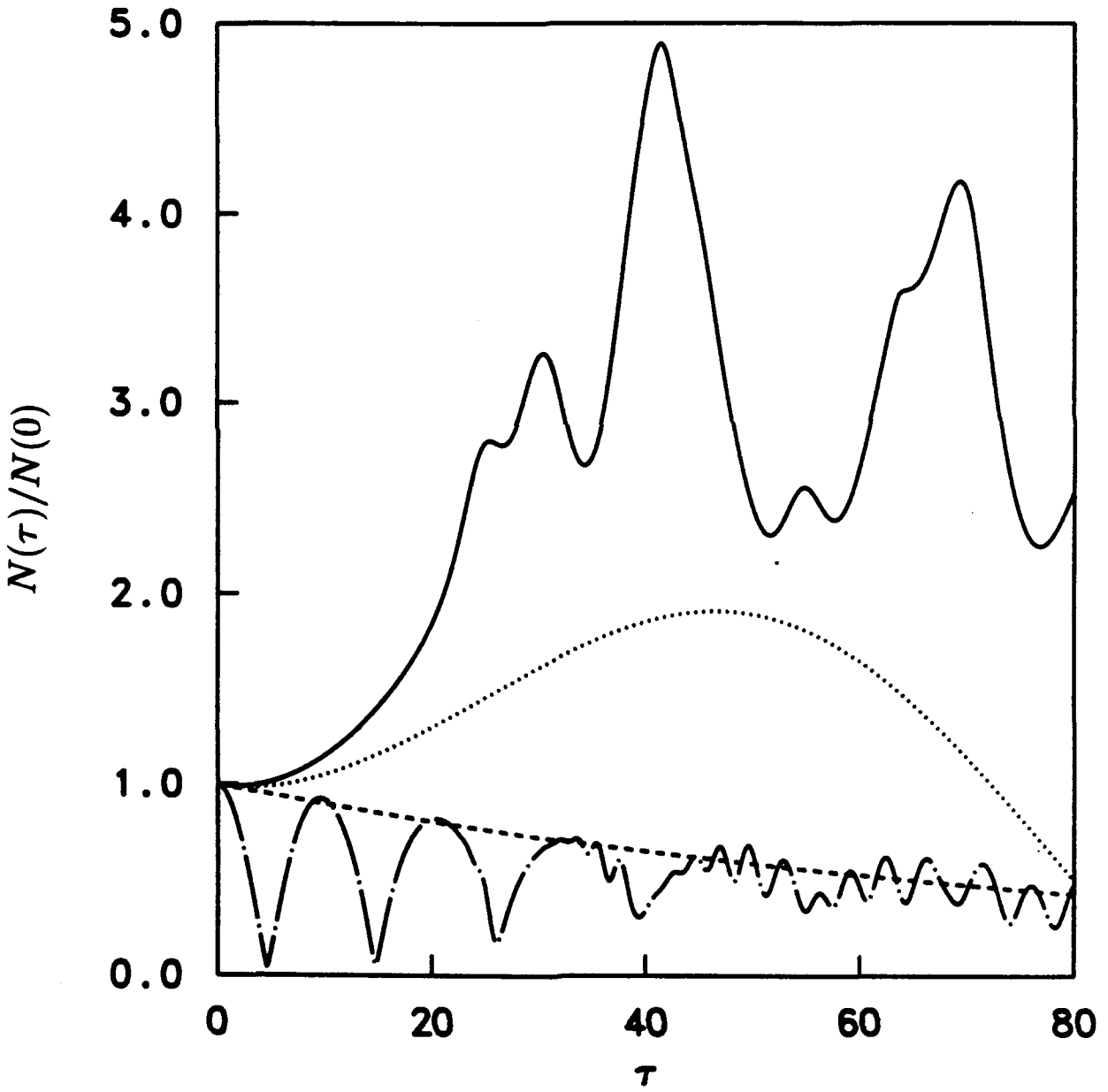

Fig. 7a

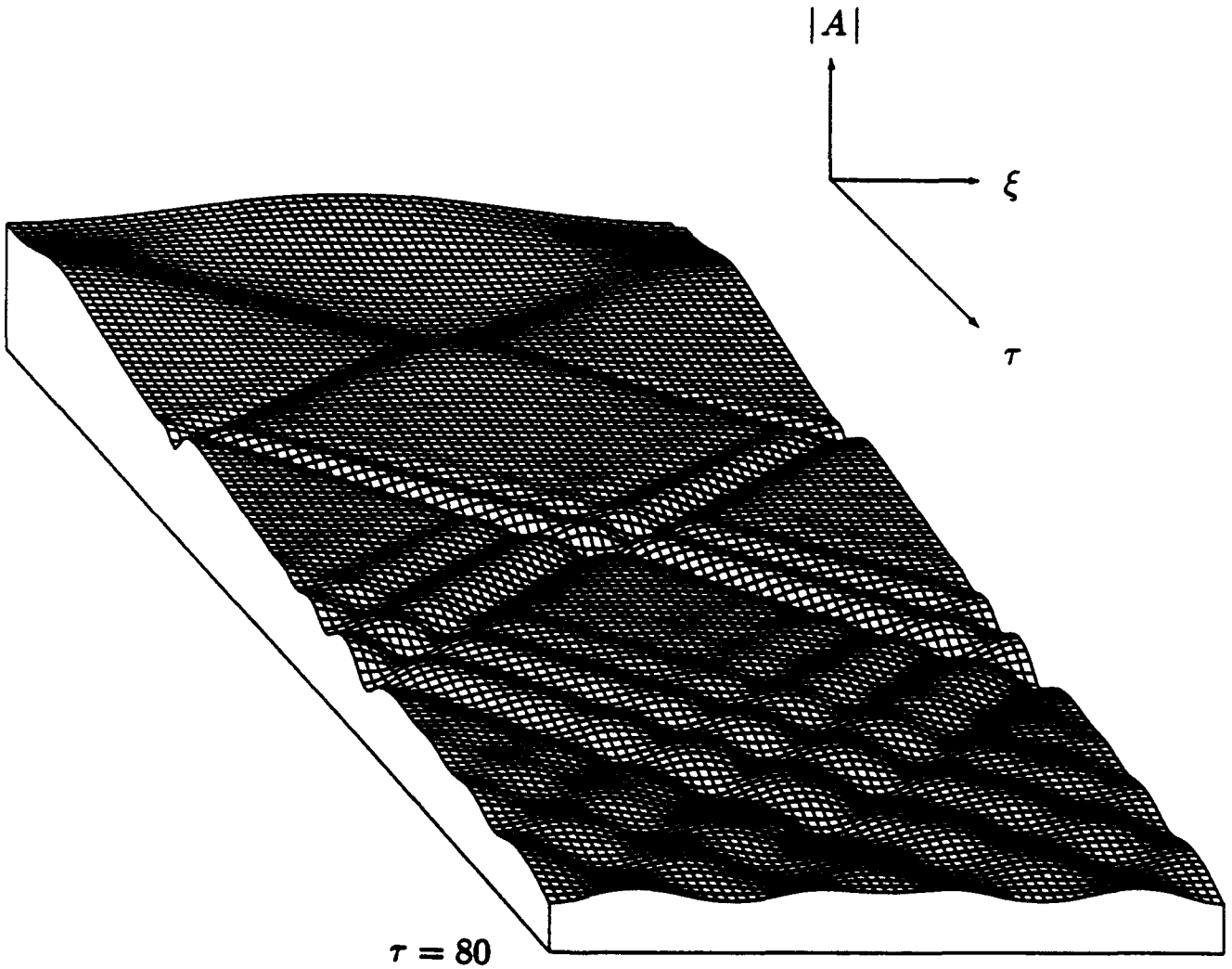

Fig 7b

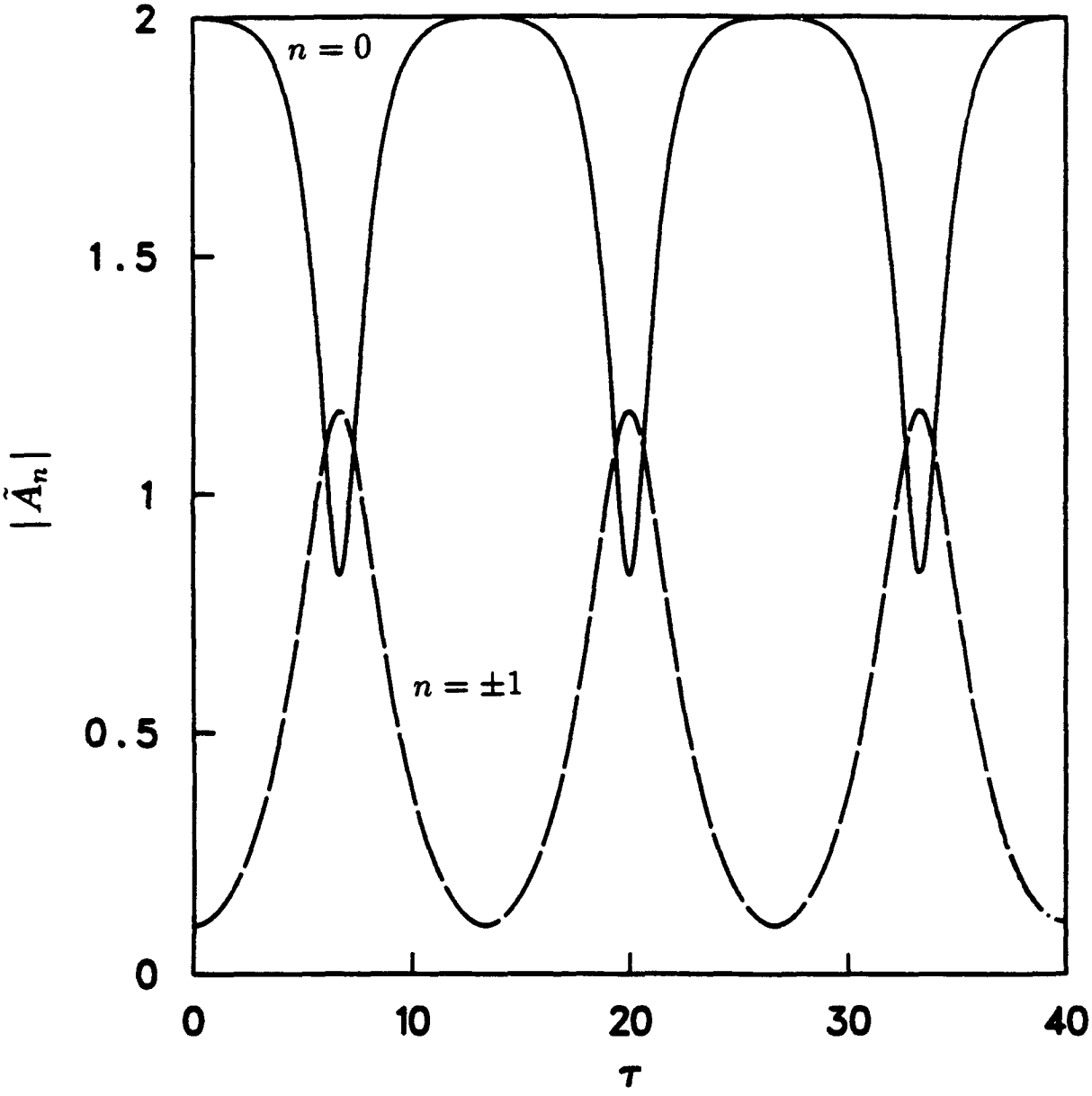

Fig 8a

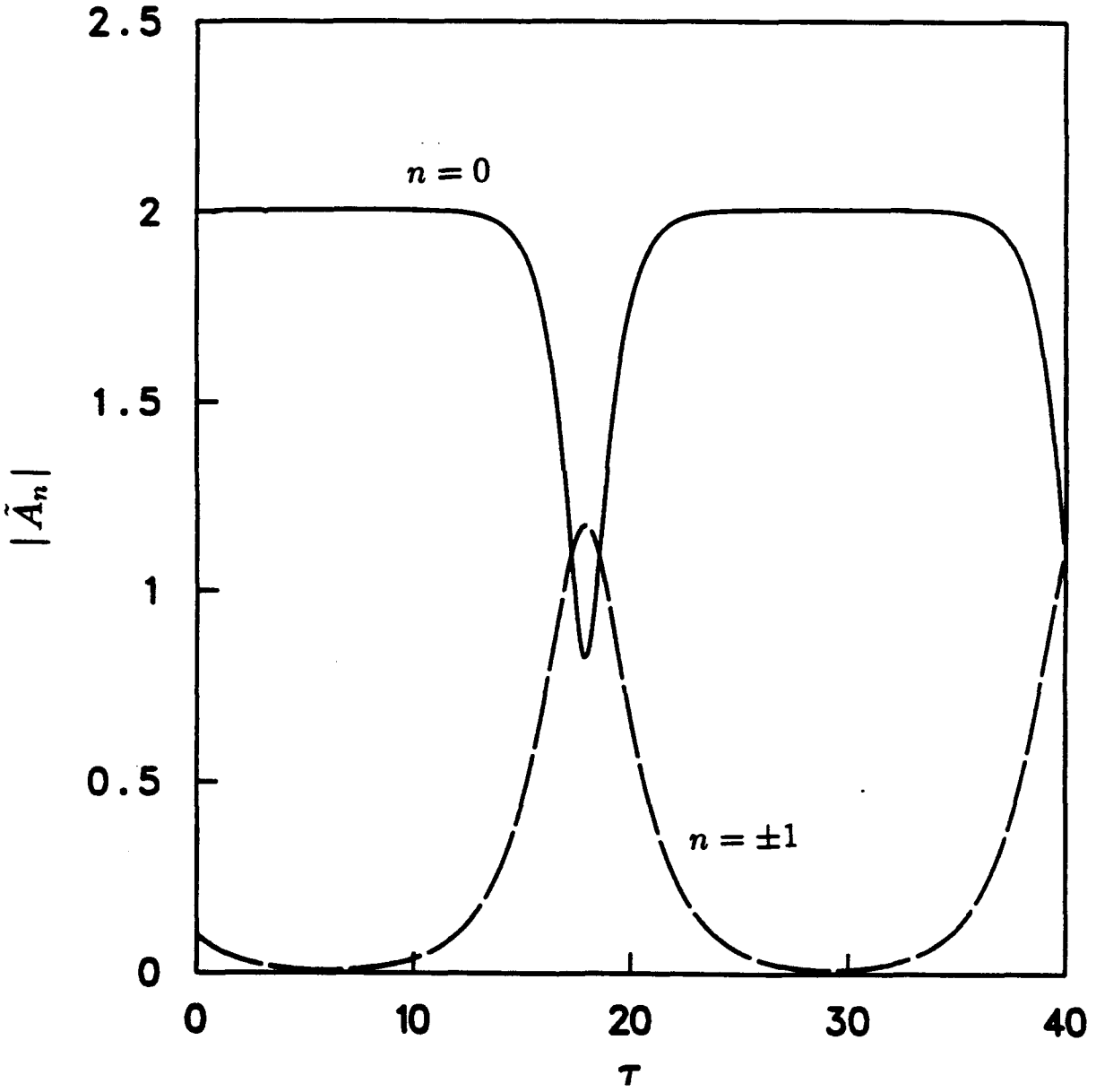

Fig 8b

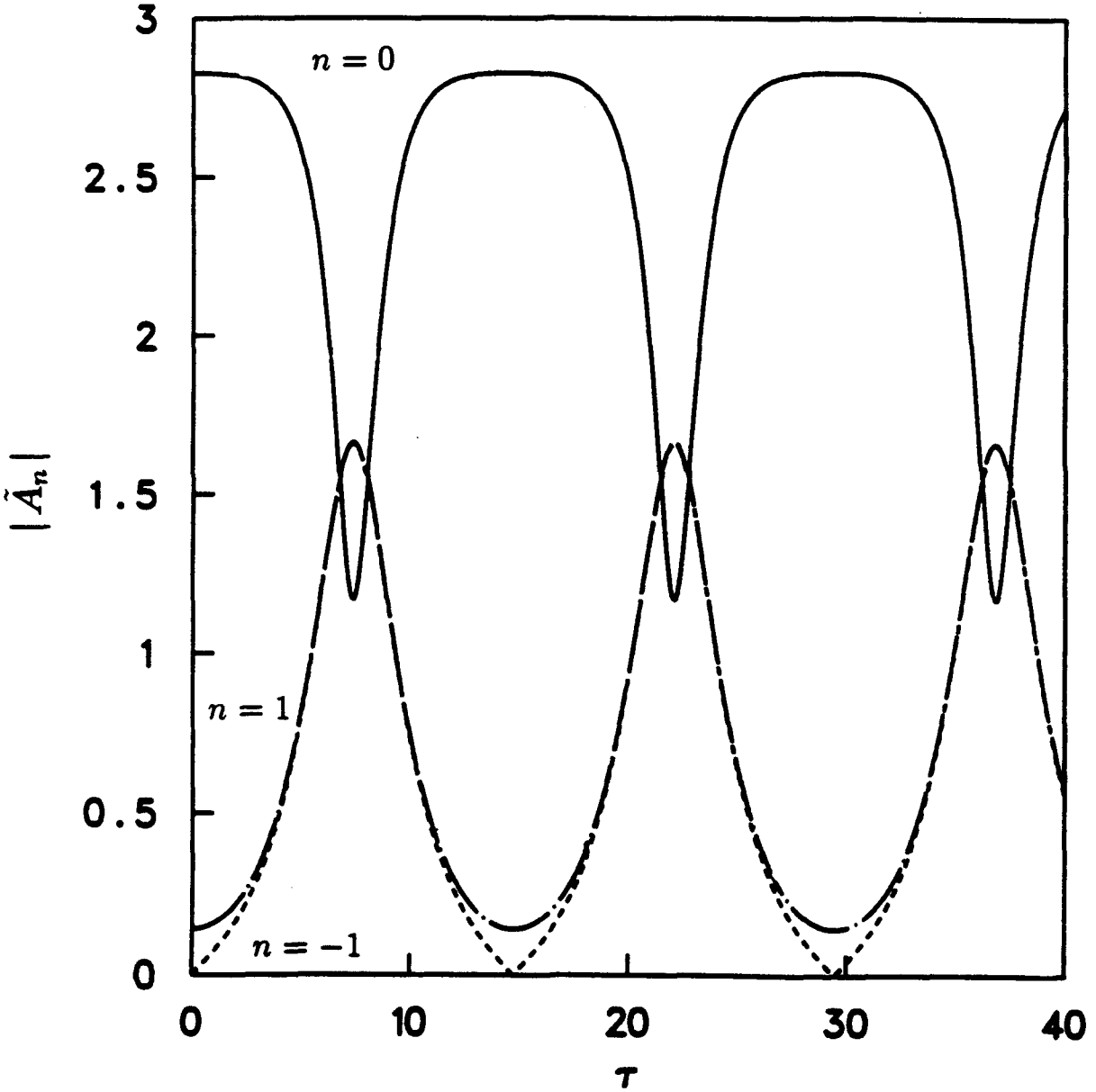

Fig 8C